

A New WIMP Population in the Solar System and New Signals for Dark-Matter Detectors

Thibault Damour

*Institut des Hautes Etudes Scientifiques, 91440 Bures-sur-Yvette, France
and DARC, Observatoire de Paris-CNRS, F-92195 Meudon, France*

Lawrence M. Krauss

*Departments of Physics and Astronomy, Case Western Reserve University
10900 Euclid Ave. Cleveland OH 44106-7079*

Abstract

We describe in detail how perturbations due to the planets can cause a sub-population of WIMPs captured by scattering in surface layers of the Sun to evolve to have orbits that no longer intersect the Sun. We argue that such WIMPs, if their orbit has a semi-major axis less than 1/2 of Jupiter's, can persist in the solar system for cosmological timescales. This leads to a new, previously unanticipated WIMP population intersecting the Earth's orbit. The WIMP-nucleon cross sections required for this population to be significant are precisely those in the range predicted for SUSY dark matter, lying near the present limits obtained by direct underground dark matter searches using cryogenic detectors. Thus, if a WIMP signal is observed in the next generation of detectors, a potentially measurable signal due to this new population must exist. This signal, lying in the keV range for Germanium detectors, would be complementary to that of galactic halo WIMPs. A comparison of event rates, anisotropies, and annual modulations would not only yield additional confirmation that any claimed signal is indeed WIMP-based, but would also allow one to gain information on the nature of the underlying dark matter model.

I. INTRODUCTION

It is by now firmly established that the dynamics of galaxies and clusters of galaxies is governed by the existence of large amounts of dark matter, with an average density sufficient to result in a total mass density in excess of 10% of the closure density today [1]. At the same time, constraints from Big Bang Nucleosynthesis [2–4] suggest that the abundance of baryons, including dark baryons, is not likely to be sufficient to account for all of this material. Thus, one is led to the possibility of non-baryonic dark matter, composed of a dissipationless gas of very weakly interacting elementary particles. The data from structure

formation also suggests that most of the dark matter must be “cold”, namely non-relativistic at the time fluctuations on the scale of galaxies first could begin to condense.

For these reasons, a favored candidate for dark matter is a so-called WIMP, Weakly Interacting Massive Particle. The best motivated among the possibilities involves supersymmetric extensions of the standard model. In these models, the lightest supersymmetric partner of ordinary particles, usually the neutralino, can be absolutely stable. Moreover, in order to resolve various naturalness problems in the Standard Model, the mass scale of the neutralino is expected to be comparable to the weak symmetry breaking scale. As a result, there is a dynamical argument that naturally leads to a remnant neutralino WIMP abundance comparable to the closure density today. (e.g. see [5]): The fraction of the closure density provided by cold relics left over after out-of-equilibrium annihilation of an initially thermal distribution of particles, say X , is on the order of $m_X n_X / \rho_{\text{closure}} = \Omega_X \sim 10^{-37} \text{ cm}^2 h^{-2} / \langle \sigma_a(v/c) \rangle$ where σ_a is the annihilation cross section (and where $\Omega_X \equiv \rho_X / \rho_{\text{closure}}$, and $h \equiv H_0 / 100 \text{ km/s/Mpc}$) [5,6]. As a result, the typical annihilation cross section needed for leaving a density of massive relics comparable to the closure density is a *weak scale* cross section: $\alpha^2 (100 \text{ GeV})^{-2} \sim (\alpha / 10^{-2})^2 \times 4 \times 10^{-36} \text{ cm}^2$. In this paper, we shall assume that the dark matter is indeed made of such weakly interacting massive particles (WIMPs). Though most of our work depends only on the general assumption of WIMPs (with mass $10 \text{ GeV} < m_X < 1000 \text{ GeV}$), we shall give numerical estimates for the effects we discuss by sampling the parameter space of the Minimal Supersymmetric Standard Model (MSSM) in its various forms [5].

Several searches for these WIMPs are underway, using either direct (energy deposition in laboratory samples) or indirect (e.g. looking for products of WIMP annihilation) techniques. Direct searches look for recoil events (with associated phenomena such as heat deposition, ionisation, etc.) due to the elastic scattering of WIMPs on nuclei. These searches present many experimental challenges because: (i) the rate of expected signals is small (less than a few events/day/kg), (ii) the recoil energies are also small (typically from 1 to 30 keV), and (iii) the background rate is comparatively very high.

Any *a priori* theoretical information on the expected signals is therefore very important for separating true signals from background events. In the present paper, we shall describe in detail the derivation and characteristics of our previously announced result [7] that a heretofore unexplored aspect of the dynamical history of WIMPs in the solar system may lead to a new population of WIMPs whose signals lead to a peculiar signature in the differential energy spectrum of recoil events, and, probably, peculiar anisotropy and annual modulation features. The new signals discussed here correspond to an excess of recoil events in an energy window on the keV energy scale. The ratio of the rate of these events (per day, per kg and per keV) to the standardly expected one is proportional to an average scattering cross section of the WIMP, weighted over elements in the Sun. Sampling over SUSY parameter space, we find that this event rate ratio can be larger than a factor of 2. Most important perhaps, we find that it is for cross sections that lie just below current experimental limits, namely for those WIMPs that are the prime target of the next generation of underground detectors, that the new signal we describe is maximal. Hence, if WIMPs are discovered in the next generation of detectors, the signal we propose may be one of the best ways of demonstrating its origin, and probing the characteristics of the WIMP dark matter responsible for it. Finally, another signal associated to the new dynamical class of WIMPs that we discuss here might be a

significant increase in the (indirect) neutrino signal expected from WIMP annihilations in the Earth. Indeed, limits from such searches might possibly further constrain the region of SUSY dark matter parameters that remain viable.

The outline of this paper is as follows: First, we derive in section II the differential capture rate by the Sun for WIMPs that might eventually form part of the population of interest here. Next (section III), we derive in detail the dynamical equations that govern the possible diffusion of this population into bound solar system orbits that no longer intersect the Sun. In the next section, we combine the results of the two preceding discussions to estimate the capture rate of long-surviving solar-system bound WIMPs. Based on this, we can then estimate (in section V) the present phase-space distribution of such WIMPs in the region of the Earth. We are then able, in section VI, to explore the possible observable signals from this new population, in terms of the differential event rate per kg per day per keV of scattering on target nuclei. In section VII we explore these results in the context of realistic SUSY WIMPs. By sampling the allowed SUSY phase space, using accelerator constraints, and using the “Neutdriver” code [5] to determine remnant WIMP densities and calculate capture and scattering cross sections on various targets, we demonstrate that the direct scattering signal from this new population should in principle be detectable if WIMPs lie near the current bounds. Finally, in the concluding section we examine other possible signatures for this distribution, and discuss future work that would be useful to perform in light of the results we present here.

II. DIFFERENTIAL CAPTURE OF WIMPS BY THE SUN

Direct searches of WIMPs assume that the recoil events are due to the scattering on a nucleus of a WIMP coming directly from a “standard” galactic halo, with a local mass density (around the solar system) $\rho_X \sim 0.3 \text{ GeV/cm}^3$, and a roughly Maxwellian velocity distribution (in the galactic inertial frame) characterized by $v_{\text{rms}} \sim 270 \text{ km/sec}$. In this paper, we shall study a particular class of WIMPs that underwent the following dynamical history:

- (i) coming from the galactic halo, they are scattered by nuclei in the outskirts of the Sun into very elliptic, bound orbits with semi-major axis $a \sim 1$ astronomical unit (AU);
- (ii) being perturbed by gravitational interaction with the planets, they diffuse out of the Sun and stay bound in the inner solar system during its entire age, $t_S \sim 4.5 \text{ Gyr}$;
- (iii) finally, they form a class of low velocity WIMPs, with typical barycentric velocities $v_X \sim v_{\text{Earth}} \sim 30 \text{ km/s}$, which can either undergo a scattering event with a nucleus in a dark-matter detector, or be scattered by a nucleus in the Earth to be ultimately accreted to finally annihilate at the Earth’s center.

In this Section, we consider the first step of this process: the scattering by nuclei in the Sun into an AU-scale bound orbit. The essential new feature with respect to previous analyses of capture of WIMPs by the Sun [8–10] will be to concentrate on WIMPs that *graze the Sun*, and lose just enough energy to stay in Earth-crossing orbits. To estimate the number of WIMPs susceptible to be sufficiently perturbed by the small gravitational interaction of planets, we need first to derive the *differential* capture rate, per energy and per angular momentum, of WIMPs by the Sun. We shall ultimately be interested only in the

small fraction of WIMPs which have angular momenta in a small range $J_{\min} \leq J \leq J_S$ where J_S is the angular momentum for a WIMP exactly grazing the Sun. The result we need is a simple generalization of results previously derived in the literature [9,10]. However, for the benefit of the general reader we shall present a self-contained derivation starting essentially from scratch.

Let

$$dn_X = f_\infty(\mathbf{v}_\infty) d^3 \mathbf{x}_\infty d^3 \mathbf{v}_\infty = f_{\text{loc}}(\mathbf{x}_{\text{loc}}, \mathbf{v}_{\text{loc}}) d^3 \mathbf{x}_{\text{loc}} d^3 \mathbf{v}_{\text{loc}}, \quad (2.1)$$

be the phase-space distribution of WIMPs, at infinity (in the galactic halo), and locally within the solar system. We shall always refer WIMP velocities to a frame attached to the Sun. Let \mathbf{v}_S denote the (vectorial) velocity of the Sun with respect to a galactic frame. The galactic WIMP velocity would be $\mathbf{v}'_{\text{WIMP}} = \mathbf{v}_{\text{WIMP}} + \mathbf{v}_S$. The distribution function at infinity is taken to be Maxwellian,

$$f_\infty(\mathbf{v}_\infty) = \frac{n_X}{\pi^{3/2} v_o^3} \exp\left(-\frac{(\mathbf{v}_\infty + \mathbf{v}_S)^2}{v_o^2}\right) \quad (2.2)$$

where $v_o^2 \equiv \frac{2}{3} v_{\text{rms}}'^2 \equiv \frac{2}{3} \langle \mathbf{v}'_\infty{}^2 \rangle$ is an rms “planar” velocity. As the class of WIMPs studied here does not depend much on any eventual cut-off of f_∞ beyond some “evaporation” velocity, we shall work with the simple exponential form (2.2). In the body of the text we shall assume the following standard values for the parameters $\rho_X = n_X m_X$, v_o , and v_S :

$$\rho_X^{\text{standard}} = n_X m_X = 0.3 \text{ GeV cm}^{-3}, \quad v_o^{\text{standard}} = 220 \text{ kms}^{-1}, \quad v_S = 220 \text{ kms}^{-1}. \quad (2.3)$$

At the end, we shall comment on the effect of changes around the standard values for ρ_X and v_o .

Liouville’s theorem tells us that $f_{\text{loc}}(\mathbf{x}_{\text{loc}}, \mathbf{v}_{\text{loc}})$ is constant along the free motion of WIMPs. Therefore, at any point along an incoming trajectory

$$f_{\text{loc}}(\mathbf{x}_{\text{loc}}, \mathbf{v}_{\text{loc}}) = f_\infty[\mathbf{v}_\infty(\mathbf{x}_{\text{loc}}, \mathbf{v}_{\text{loc}})], \quad (2.4)$$

where $\mathbf{v}_\infty(\mathbf{x}_{\text{loc}}, \mathbf{v}_{\text{loc}})$ is the incoming velocity at infinity of the WIMP observed locally, at position \mathbf{x}_{loc} , with velocity \mathbf{v}_{loc} , within the solar system (before it undergoes any scattering event). In spherically symmetric problems, only the angular average $\bar{f}_{\text{loc}}(\mathbf{x}_{\text{loc}}, \mathbf{v}_{\text{loc}}) = \bar{f}_\infty[v_\infty(\mathbf{x}_{\text{loc}}, \mathbf{v}_{\text{loc}})]$ matters, with

$$\bar{f}_\infty(v_\infty) = \frac{n_X}{4 \pi^{3/2} v_o v_S v_\infty} \left[e^{-\left(\frac{v_\infty - v_S}{v_o}\right)^2} - e^{-\left(\frac{v_\infty + v_S}{v_o}\right)^2} \right]. \quad (2.5)$$

It is standard to write the differential scattering cross-section of the WIMP X onto the nucleus of atomic number A as

$$d\sigma_A = \sigma_A F_A^2(Q) \frac{d\Omega_{\text{cm}}}{4\pi}, \quad (2.6)$$

where $Q = E_{\text{before}} - E_{\text{after}}$ is the energy transferred during the scattering, $F_A(Q)$ is a form factor, and $d\Omega_{\text{cm}} = \sin\theta_{\text{cm}} d\theta_{\text{cm}} d\varphi_{\text{cm}}$ is the scattering solid angle element *in the center of mass* frame. We shall take an exponential form factor

$$F^2(Q) = \exp(-Q/Q_A), \quad (2.7)$$

where the nucleus-dependent quantity Q_A will be discussed below. Note that σ_A (often denoted σ_A^0) in Eq. (2.6) is by definition independent of the scattering angle.

Let us consider a volume element $d^3\mathbf{x}$ in the Sun, containing $n_A(\mathbf{x}) d^3\mathbf{x}$ nuclei of atomic number A . The differential *flux* of WIMPs impinging on this lump of scatterers is $d^3\mathbf{v}_{\text{loc}} f_{\text{loc}}(\mathbf{x}, \mathbf{v}_{\text{loc}}) |\mathbf{v}_{\text{loc}}|$. Therefore, the corresponding differential number per second of scattering events (within the center-of-mass scattering solid angle $d\Omega_{\text{cm}}$) reads

$$d\dot{N}_A = d^3\mathbf{x} n_A(\mathbf{x}) d^3\mathbf{v}_{\text{loc}} f_{\text{loc}}(\mathbf{x}, \mathbf{v}_{\text{loc}}) |\mathbf{v}_{\text{loc}}| \sigma_A F_A^2(Q) \frac{d\Omega_{\text{cm}}}{4\pi}. \quad (2.8)$$

We wish to sort out this scattering rate according to the distribution in outgoing semi-major axis a and (specific) angular momentum J . The conserved energy (kinetic plus potential) of the WIMP before the scattering event is

$$E_{\text{before}} = \frac{1}{2} m_X (\mathbf{v}_{\text{loc}}^2 - v_{\text{esc}}^2(r)) = \frac{1}{2} m_X \mathbf{v}_{\infty}^2, \quad (2.9)$$

where $\mathbf{v}_{\text{loc}} \equiv \mathbf{v}_{\text{before}}$ denotes the local velocity before the collision, and where $v_{\text{esc}}^2(r) \equiv 2U(r) \equiv +2 \int d^3\mathbf{x}' G_N \rho(\mathbf{x}') / |\mathbf{x} - \mathbf{x}'|$ is the escape velocity at the radius r within the Sun (G_N denoting the Newtonian gravitational constant). The conserved energy after the collision reads

$$E_{\text{after}} = \frac{1}{2} m_X (\mathbf{v}_{\text{after}}^2 - v_{\text{esc}}^2(r)) = -\frac{G_N m_X M_{\odot}}{2a} \equiv -\frac{1}{2} m_X \alpha, \quad (2.10)$$

where M_{\odot} denotes the mass of the Sun, and where α is a shorthand for $G_N M_{\odot}/a$. By the standard laws of nonrelativistic elastic collisions (see, e.g., [11]), the velocity after the collision, and therefore the energy transfer, are linked to the c.m. scattering angle θ_{cm} by

$$\mathbf{v}_{\text{after}}^2 = \mathbf{v}_{\text{loc}}^2 \left[1 - \frac{1}{2} \beta_+^A (1 - \cos \theta_{\text{cm}}) \right], \quad Q = E_{\text{before}} - E_{\text{after}} = \frac{1}{2} m_X \beta_+^A \mathbf{v}_{\text{loc}}^2 \frac{1 - \cos \theta_{\text{cm}}}{2}, \quad (2.11)$$

where we define (following Ref. [5])

$$\beta_{\pm}^A \equiv \frac{4 m_X m_A}{(m_X \pm m_A)^2}. \quad (2.12)$$

Note that the maximum value of β_+^A is one, which is reached when the mass of the WIMP matches the mass of the nucleus: $m_X = m_A$. For a given incoming local velocity \mathbf{v}_{loc} , Eqs. (2.9), (2.10) give

$$Q = \frac{1}{2} m_X (v_{\text{loc}}^2 - v_{\text{esc}}^2(r) + \alpha) = \frac{1}{2} m_X (v_{\infty}^2 + \alpha). \quad (2.13)$$

On the other hand, Eq. (2.11) relates the energy transfer Q to the c.m. scattering solid angle. Finally, we have

$$\frac{d\Omega_{\text{cm}}}{4\pi} = d\left(\frac{1 - \cos\theta_{\text{cm}}}{2}\right) = \frac{dQ}{\frac{1}{2} m_X \beta_+^A v_{\text{loc}}^2} = \frac{d\alpha}{\beta_+^A v_{\text{loc}}^2}, \quad (2.14)$$

where we recall that $\alpha \equiv G_N M_\odot/a$.

Inserting Eq. (2.14) in Eq. (2.8) yields

$$d\dot{N}_A = d^3\mathbf{x} n_A(\mathbf{x}) \sigma_A \frac{d^3\mathbf{v}_{\text{loc}} f_{\text{loc}}(\mathbf{x}, \mathbf{v}_{\text{loc}})}{\beta_+^A v_{\text{loc}}} F_A^2(Q) d\alpha \Theta_\alpha, \quad (2.15)$$

where the last factor is a step function ($\Theta(x) \equiv 1$ if $x \geq 0$, and vanishes if $x < 0$) taking care of the inequality on v_{loc} or $v_\infty^2(\mathbf{x}, \mathbf{v}_{\text{loc}}) = v_{\text{loc}}^2 - v_{\text{esc}}^2(r)$ entailed by the constraint $(1 - \cos\theta_{\text{cm}})/2 \leq 1$, i.e. $2Q/m_X = v_\infty^2 + \alpha \leq \beta_+^A v_{\text{loc}}^2 = \beta_+^A (v_\infty^2 + v_{\text{esc}}^2(r))$. Using the identity $(1/\beta_+^A) - (1/\beta_-^A) \equiv 1$, easily checked from the definitions (2.12), this constraint leads to the step function

$$\Theta_\alpha \equiv \Theta \left[\beta_-^A \left(v_{\text{esc}}^2(r) - \frac{\alpha}{\beta_+^A} \right) - v_\infty^2 \right]. \quad (2.16)$$

The phase-space distribution of the WIMPs at infinity, Eq. (2.2), is anisotropic. If the overall capture mechanism discussed in this paper were spherically symmetric (i.e. a capture by a spherical Sun followed by a spherically symmetric exit mechanism), it would be exact to replace, for purposes of capture calculations, the (anisotropic) incoming phase-space distribution, Eq. (2.2), by its (isotropic) angular average, Eq. (2.5). Actually, the overall capture mechanism discussed here is not spherically symmetric (even in the (excellent) approximation of an exactly spherical Sun), because, as we shall see in the next section, two angular parameters (i and g), related to the spatial orientations of $\mathbf{v}_{\text{after}}$ and \mathbf{x} with respect to the ecliptic plane, modulate the efficiency of extraction of the WIMPs captured by the Sun. However, we expect that, because of the partial randomisation of the incoming directional quantities by scattering on a spherical Sun, the effects linked to the overall lack of spherical symmetry, i.e. the correlation effects between the incoming anisotropy (linked to the direction of \mathbf{v}_S) and the outgoing one (linked to the ecliptic plane) are small. Therefore, we shall henceforth neglect them, for purposes of capture calculations, and replace the anisotropic distribution, Eq. (2.2), by its angular average, and, correspondingly, the local distribution $f_{\text{loc}}(\mathbf{x}, \mathbf{v}_{\text{loc}})$ by its angular average \bar{f}_{loc} , which, thanks to Liouville's theorem (2.4), is simply equal to $\bar{f}_\infty[v_\infty(r, v_{\text{loc}})]$. We can then make use of the spherical symmetry of \bar{f}_{loc} and $n_A(\mathbf{x}) = n_A(r)$ to simplify the problem of sorting out the differential rate (2.15) according to the distribution in the outgoing (specific) angular momentum $J = |\mathbf{x} \times \mathbf{v}_{\text{after}}|$. (We thank A. Gould for suggesting this simplification). Let θ denote the colatitude of $\mathbf{v}_{\text{after}}$ with respect to the radial direction taken as z -axis, i.e. $J = r v_{\text{after}} \sin\theta$. Since an isotropic distribution is uniform in $\cos\theta$, and $J \propto \sin\theta$, the distribution in J^2 is given by the normalized measure

$$dJ^2 (2J_{\text{max}}^2)^{-1} (1 - J^2/J_{\text{max}}^2)^{-1/2} \Theta_J, \quad (2.17)$$

where

$$J_{\text{max}}(r, \alpha) \equiv r(v_{\text{esc}}^2(r, \alpha) - \alpha)^{1/2} = r v_{\text{after}}, \quad \Theta_J \equiv \Theta(J_{\text{max}}(r, \alpha) - J). \quad (2.18)$$

Here, the theta function Θ_J takes care of the constraint $\sin \theta < 1$. This leads to a differential scattering rate of the form

$$d\dot{N}_A = d^3\mathbf{x} n_A(r) \sigma_A \frac{4\pi v_{\text{loc}} dv_{\text{loc}} \bar{f}_{\text{loc}}(r, v_{\text{loc}})}{2J_{\text{max}}^2 \beta_+^A} \left(1 - \frac{J^2}{J_{\text{max}}^2}\right)^{-1/2} F_A^2(Q) \Theta_\alpha \Theta_J d\alpha dJ^2. \quad (2.19)$$

Performing the integral over J in Eq. (2.19) over the range $J_{\text{min}} \leq J \leq J_{\text{max}}$ leads to

$$d\dot{N}_A|_{J \geq J_{\text{min}}} = d^3\mathbf{x} n_A(r) \sigma_A \left(1 - \frac{J_{\text{min}}^2}{(J_{\text{max}}(r, \alpha))^2}\right)^{1/2} \Theta_{J_{\text{min}}} \frac{4\pi v_{\text{loc}} dv_{\text{loc}} \bar{f}_{\text{loc}}}{\beta_+^A} F_A^2(Q) \Theta_\alpha d\alpha, \quad (2.20)$$

in which Q should be replaced by its expression in terms of v_{loc}^2 or v_∞^2 , Eq. (2.13). Here, $\Theta_{J_{\text{min}}} = \Theta[r v_{\text{after}} - J_{\text{min}}] = \Theta[J_{\text{max}}(r, \alpha) - J_{\text{min}}]$ gives a lower bound to the admissible values of $r = |\mathbf{x}|$. The integrals over $d^3\mathbf{x} = 4\pi r^2 dr$ and dv_{loc} are uncoupled. Using the exponential form factor (2.7) we then define the function

$$\begin{aligned} K_A(r, \alpha) &\equiv \frac{v_o}{n_X} \frac{1}{\beta_+^A} \int 4\pi v_{\text{loc}} dv_{\text{loc}} \bar{f}_{\text{loc}} \exp\left[-\frac{m_X}{2Q_A} (v_{\text{loc}}^2 - v_{\text{esc}}^2(r) + \alpha)\right] \Theta_\alpha \\ &\equiv \frac{v_o}{n_X} \frac{1}{\beta_+^A} \int 4\pi v_\infty dv_\infty \bar{f}_\infty(v_\infty) \exp\left[-\frac{m_X}{2Q_A} (v_\infty^2 + \alpha)\right] \Theta_\alpha. \end{aligned} \quad (2.21)$$

In the second form, simplified by taking $v_\infty(r, v_{\text{loc}}) = (v_{\text{loc}}^2 - v_{\text{esc}}^2(r))^{1/2}$ as integration variable, we used $v_{\text{loc}} dv_{\text{loc}} = v_\infty dv_\infty$ and Liouville's theorem. Note that the step function Θ_α limits v_∞^2 to the range $0 \leq v_\infty^2 \leq \beta_-^A (v_{\text{esc}}^2(r) - \alpha/\beta_+^A)$. With the definition (2.21), the result (2.20) can be finally written as (after integration over the Sun)

$$\left.\frac{d\dot{N}_A}{d\alpha}\right|_{J \geq J_{\text{min}}} = \frac{n_X}{v_o} \int_{r \geq r_{\text{min}}} d^3\mathbf{x} n_A(r) \sigma_A \left(1 - \frac{J_{\text{min}}^2}{r^2 (v_{\text{esc}}^2(r) - \alpha)}\right)^{1/2} K_A(r, \alpha). \quad (2.22)$$

Evidently, the sum over all the (significant) values of A (atomic number) present in the Sun must be ultimately performed. Here, the minimum radius r_{min} (perihelion distance) is defined in terms of the minimum angular momentum J_{min} by $r_{\text{min}} (v_{\text{esc}}^2(r_{\text{min}}) - \alpha)^{1/2} \equiv J_{\text{min}}$. This formula yields the result needed for our purpose. Namely, the rate with which WIMPs scatter on nuclei with atomic number A to end up into bound solar orbits with semi-major axis within $[a, a + da]$ (corresponding to $[\alpha, \alpha + d\alpha]$ with $a \equiv G_N M_\odot/a$), and with specific angular momentum $J \geq J_{\text{min}}$.

The limit $J_{\text{min}} \rightarrow 0^+$ would collect all the WIMPs scattered at any point within the Sun, even with very small perihelion distances r_{min} , i.e. passing very near the center of the Sun. In our subsequent work we shall be interested in the opposite limit $J_{\text{min}} \rightarrow (R_S v_{\text{esc}}(R_S))^-$ corresponding to orbits which graze the Sun (radius R_S) and barely penetrate it. The usual total capture rate is obtained from Eq. (2.22) by setting $J_{\text{min}} = 0$ and by integrating over $\alpha = GM_\odot/a$. We shall be interested in values $J_{\text{min}} \simeq R_S v_{\text{esc}}(R_S)$ and $a \sim 1 \text{ AU}$, i.e. $\alpha \sim GM_\odot/(1 \text{ AU}) \sim v_E^2$ where $v_E = 29.8 \text{ km/s}$ is the Earth orbital velocity. Note that for such values of a , $v_{\text{esc}}^2 \gg \alpha$ so that we can, with a very good approximation, neglect

α with respect to v_{esc}^2 both in the square-root factor in Eq. (2.22) and in the definition of r_{min} : $r_{\text{min}} v_{\text{esc}}(r_{\text{min}}) \simeq J_{\text{min}}$. Further, for Sun-grazing orbits we can approximate the radial dependence of the escape velocity by: $v_{\text{esc}}^2(r) \simeq 2GM_{\odot}/r$. Within these approximations, the differential rate $[d\dot{N}_A/d\alpha]_{J_{\text{min}}}$ reads

$$\left. \frac{d\dot{N}_A}{d\alpha} \right|_{J \geq J_{\text{min}}} \simeq \frac{n_X}{v_o} \int_{r \geq r_{\text{min}}} d^3\mathbf{x} n_A(r) \sigma_A \left(1 - \frac{r_{\text{min}}}{r}\right)^{1/2} K_A(r, \alpha). \quad (2.23)$$

Note also that for the values of a we are interested in, typically $\alpha \sim v_E^2 \ll v_{\infty}^2$, so that the function $K_A(r, \alpha)$ is nearly independent of α . Let us finally write more explicitly the result (2.21). Inserting the explicit (angle-averaged) shifted Maxwellian spectrum (2.5) into Eq. (2.21), one can express K_A in terms of the error function

$$\chi(x) \equiv \int_0^x dy e^{-y^2} \equiv \frac{\pi^{1/2}}{2} \text{erf}(x). \quad (2.24)$$

To do this one must use as integration variable $x \equiv \sqrt{1 + \hat{a}_A} v_{\infty}/v_o$ (where \hat{a}_A is defined below). Setting

$$\hat{a}_A \equiv \frac{m_X v_o^2}{2Q_A}, \quad \eta_a \equiv \frac{1}{\sqrt{1 + \hat{a}_A}} \frac{v_S}{v_o}, \quad (2.25)$$

and, with $A(r) > 0$,

$$(A(r))^2 \equiv (1 + \hat{a}_A) \frac{\beta_-^A}{v_o^2} \left(v_{\text{esc}}^2(r) - \frac{\alpha}{\beta_+^A} \right), \quad (2.26)$$

yields

$$K_A(r, \alpha) = \frac{\exp\left(-\frac{m_X \alpha}{2Q_A}\right) \exp(-\eta_a^2 \hat{a}_A)}{\pi^{1/2} \beta_+^A (1 + \hat{a}_A) \eta_a} \left[\chi(A(r) - \eta_a) - \chi(A(r) + \eta_a) + 2\chi(\eta_a) \right]. \quad (2.27)$$

In the applications below we shall use the standard value for the coherence energy Q_A [5]

$$Q_A = \frac{3\hbar^2}{2m_A R_A^2}, \quad R_A = 10^{-13} \text{ cm} \left[0.3 + 0.91 \left(\frac{m_A}{\text{GeV}} \right)^{\frac{1}{3}} \right]. \quad (2.28)$$

When one can neglect both the form factor ($Q_A \rightarrow \infty$) and the relative velocity of the Sun with respect to the galactic halo ($\eta_a \rightarrow 0$), Eq. (2.27) simplifies to the form given in [7]

$$K_A(r, \alpha)|_{\eta_a=0}^{Q_A=\infty} = \frac{2}{\pi^{1/2}} \frac{1}{\beta_+^A} \left[1 - \exp \left[-\frac{\beta_-^A}{v_o^2} \left(v_{\text{esc}}^2(r) - \frac{\alpha}{\beta_+^A} \right) \right] \right]. \quad (2.29)$$

III. GETTING SOME OF THE CAPTURED WIMPS OUT OF THE SUN

The scattering events discussed in the previous Section create a population of solar-system bound WIMPs, moving (for $a \sim 1$ AU) on very elliptic orbits that traverse the Sun again and again. For the values of WIMP-nuclei cross sections we shall be mostly interested in below (corresponding to effective WIMP-proton cross sections (see section VII) in the range $4 \times 10^{-42} - 4 \times 10^{-41}$ cm²), the mean opacity of the Sun for orbits with small perihelion distances is in the range $10^{-4} - 10^{-3}$. This means that after only $10^3 - 10^4$ orbits (i.e. $\sim 10^3 - 10^4$ yr) these WIMPs will undergo a second scattering event in the Sun, making them lose more energy, i.e. binding them even more to the Sun. From Eq. (2.11) the average energy loss per scattering is

$$\langle Q \rangle = \frac{1}{4} m_X \beta_+^A \mathbf{v}_{\text{loc}}^2 \simeq \frac{1}{4} m_X \beta_+^A v_{\text{esc}}^2(r) \simeq m_X \left(\frac{m_A}{m_X} \right) v_{\text{esc}}^2(r), \quad (3.1)$$

where we assumed $m_A \ll m_X$.

Compared to the conserved energy before this (second) scattering event, $E = -\frac{1}{2} m_X \alpha$, the mean energy loss (3.1) is quite large, because $\langle v_{\text{esc}}^2(r) \rangle_{\text{Sun}} \sim (1000 \text{ km/s})^2 \gg \frac{1}{2} \alpha \sim \frac{1}{2} v_E^2 \sim \frac{1}{2} (30 \text{ km/s})^2$. Even assuming a typical mass ratio as small as $m_{16}/1 \text{ TeV} \sim 1.6 \times 10^{-2}$ does not compensate the large factor $2 \langle v_{\text{esc}}^2 \rangle / v_E^2 \sim 2 \times 10^3$. The conclusion is that a second scattering event would typically bind the WIMP on an orbit of semi-major axis significantly smaller than 1 AU. This irreversible process ($\langle Q \rangle > 0$) leads rather quickly (a few $10^3 - 10^4$ yr) to orbits of size comparable to the Sun (at which stage one might need to take into account the thermal velocities of the nuclei in the Sun, ultimately leading to a near thermal equilibrium between WIMPs and the core of the Sun [12]).

The conclusion is that most of the population of WIMPs considered in the previous Section will end up quickly in the core of the Sun (where they will ultimately annihilate with each other, thereby generating an interesting indirect neutrino signal, see e.g. [5]). The only way to save some of these WIMPs from this early demise is to consider the fraction of WIMPs that have perihelion distances r_{min} in a small range near the radius of the Sun R_S , say $R_S(1 - \epsilon) \leq r_{\text{min}} \leq R_S$. As we argued in [7] focussing on such a subpopulation of WIMPs has two advantages: (i) they traverse only a small fraction of the mass of the Sun and therefore their lifetime on such grazing orbits is greatly increased, and (ii) during this time, the gravitational perturbations due to the planets can build up and push them on orbits that no longer cross the Sun. We now tackle the latter perturbation problem.

We first review in detail some concepts and notation of Hamiltonian dynamics. In standard position-momenta variables the Hamiltonian describing the basic interaction between a WIMP and the Sun reads ($r \equiv |\mathbf{x}|$)

$$\mathcal{H}_S(\mathbf{x}, \mathbf{p}) = \frac{1}{2} \mathbf{p}^2 - U(r), \quad (3.2)$$

where $U(r) = +G_N \int \rho(\mathbf{x}') d^3\mathbf{x}' / |\mathbf{x} - \mathbf{x}'|$ is the (spherically symmetric) Newtonian potential generated by the mass distribution of the Sun. Thanks to the equivalence principle, the mass m_X of the WIMP drops out of the problem (even when adding the perturbing influence of planets). Therefore in Eq. (3.2) and below we simplify the writing by factoring out m_X

of all quantities, i.e. by working formally with a unit-mass WIMP. Because of the spherical symmetry of Eq. (3.2) we can first introduce spherical coordinates $(r, \theta, \varphi, p_r, p_\theta, p_\varphi)$, with respect to which the problem is separable, and then work with some associated, convenient action-angle variables (“Delaunay variables”). The Jacobi time-independent action $S_E(r, \theta, \varphi)$ satisfying $\mathcal{H}_S(q_i, \partial S_0/\partial q_i) = E$, is of the form [11]

$$\begin{aligned} S_E(r, \theta, \varphi) &= S_r(r) + S_\theta(\theta) + S_\varphi(\varphi) \\ &= \int dr \sqrt{2E + 2U(r) - \frac{J^2}{r^2}} + \int d\theta \sqrt{J^2 - \frac{J_z^2}{\sin^2 \theta}} + J_z \varphi. \end{aligned} \quad (3.3)$$

Using S_E we can introduce the usual (action-angle) Delaunay variables, traditionally denoted $(L, G, H; \ell, g, h)$ [13]. The action variables L, G, H are related to E, J and J_z appearing in Eq. (3.3) through (with $p_r = dS_r/dr, p_\theta = dS_\theta/d\theta, p_\varphi = dS_\varphi/d\varphi$)

$$H \equiv \frac{1}{2\pi} \int_0^{2\pi} p_\varphi d\varphi = J_z, \quad (3.4a)$$

$$G \equiv \frac{2}{2\pi} \int_{\theta_{\min}}^{\theta_{\max}} p_\theta d\theta = J, \quad (3.4b)$$

$$L \equiv G + \frac{2}{2\pi} \int_{r_{\min}}^{r_{\max}} p_r dr = G + \frac{2}{2\pi} \int_{r_{\min}}^{r_{\max}} dr \sqrt{2E + 2U(r) - \frac{G^2}{r^2}}, \quad (3.4c)$$

where the extra factors 2 compensate for the integrations on the intervals $[\theta_{\min}, \theta_{\max}]$, $[r_{\min}, r_{\max}]$, corresponding to half a period for these variables. The angle variables (with period 2π) corresponding to L, G, H are respectively denoted ℓ, g, h . [Their meaning will be discussed further below.] In these variables the Hamiltonian depends only on L and G (as is clear from Eq. (3.4c)), $\mathcal{H}_S = \mathcal{H}_S(L, G)$, so that the general evolution equations,

$$\frac{d\ell}{dt} = +\frac{\partial \mathcal{H}}{\partial L}, \quad \frac{dg}{dt} = +\frac{\partial \mathcal{H}}{\partial G}, \quad \frac{dh}{dt} = +\frac{\partial \mathcal{H}}{\partial H}, \quad (3.5a)$$

$$\frac{dL}{dt} = -\frac{\partial \mathcal{H}}{\partial \ell}, \quad \frac{dG}{dt} = -\frac{\partial \mathcal{H}}{\partial g}, \quad \frac{dH}{dt} = -\frac{\partial \mathcal{H}}{\partial h}, \quad (3.5b)$$

tell us, in the case of the problem (3.2) that the action variables L, G and H are constant, while, among the angle variables, h is constant, but ℓ and g evolve linearly in time: $\ell = nt + \ell_o$, $g = \dot{\omega} t + g_o$. Here, $n \equiv 2\pi/P$ is the mean angular frequency of the radial motion ($P =$ perihelion to perihelion period), and $\dot{\omega}$ is the mean rate of advance of the perihelion.

The central point is the following. A WIMP orbit with a generic perihelion distance $r_{\min} \lesssim R_S$ will undergo a large perihelion precession $\Delta\omega \sim 2\pi$ per orbit, i.e. $\dot{\omega} \sim n$, because the potential $U(r)$ *within the Sun* is very modified compared to the exterior $1/r$ potential leading (by “accident”) to the absence of perihelion motion. In other words, the trajectory of the WIMP will generically be a fast advancing *rosette*. This means that *both* angles ℓ and g are *fast variables*. When adding in the small perturbing effect of the planets, i.e. when considering the total Hamiltonian,

$$\mathcal{H}_{\text{tot}} = \mathcal{H}_S(L, G) + \mathcal{H}_p(L, G, H; \ell, g, h; L_p, \dots, \ell_p, \dots), \quad (3.6)$$

where \mathcal{H}_p (which contains a small factor $\mu_p = m_{\text{planet}}/M_\odot$) is the planetary perturbation, we can work out the (first-order) *secular* effects due to the planets by averaging over the fast variables ℓ and g (as well as the mean anomalies ℓ_p of the planets). Then the first two equations (3.5b) tell us immediately that the corresponding action variables L and G are secularly constant because planetary perturbations average out to zero (e.g. $\langle dG/dt \rangle = -\langle \partial\mathcal{H}/\partial g \rangle_{\ell,g} \equiv 0$, because of the averaging over the fast angle g). As we shall see below L is essentially related to the semi-major axis a of the WIMP orbit, while G/L is related to the eccentricity e . The conclusion is that when the rosette motion is fast, planetary perturbations do not induce any secular evolution in the semi-major axis and in the eccentricity of the WIMP orbit. Therefore such WIMP orbits will necessarily traverse the Sun again and again and end up falling in its core.

A different situation arises for WIMP orbits that graze the Sun. Throughout their orbits they feel essentially a $1/r$ potential due to the Sun, so that their rosette motion will be very slow. Consequently, the variable g will be slow for them (compared to ℓ), and we cannot average on g . To tackle this problem we split the total Hamiltonian (3.6) in three parts,

$$\mathcal{H}_{\text{tot}} = \mathcal{H}_o + \mathcal{H}_1 + \mathcal{H}_p, \quad (3.7)$$

where we take as unperturbed Hamiltonian the one corresponding to a point-like Sun,

$$\mathcal{H}_o = \frac{1}{2} \mathbf{p}^2 - \frac{G_N M_\odot}{r}, \quad (3.8)$$

while the perturbations are

$$\mathcal{H}_1 = -\delta U(r), \quad \mathcal{H}_p = -\sum_p G_N m_p \left(\frac{1}{|\mathbf{x}_X - \mathbf{x}_p|} - \frac{\mathbf{x}_X \cdot \mathbf{x}_p}{|\mathbf{x}_p|^3} \right). \quad (3.9)$$

Here, $\delta U(r) \equiv U(r) - G_N M_\odot/r$ is the non $1/r$ part of the potential generated by the Sun (δU is zero when $r > R_S$ and is responsible for the rosette effect when an orbit penetrates the Sun), and \mathcal{H}_p denotes the planetary perturbations [13]. It is a sum over the planets with mass m_p and heliocentric positions \mathbf{x}_p . [The last term comes from the transformation between inertial (barycentric) coordinates and heliocentric ones.] We shall henceforth use the unperturbed Delaunay variables defined by the Hamiltonian \mathcal{H}_o (corresponding to Keplerian motion). They are explicitly given in terms of the usual elliptic elements by

$$L = \sqrt{G_N M_\odot a}, \quad G = \sqrt{G_N M_\odot a(1 - e^2)}, \quad H = \sqrt{G_N M_\odot a(1 - e^2)} \cos i, \quad (3.10a)$$

$$\ell = \text{mean anomaly}, \quad g = \omega = \text{periastron argument},$$

$$h = \Omega = \text{longitude of the ascending mode}. \quad (3.10b)$$

Here, i denotes the inclination (with respect to the ecliptic), and we recall that the mean anomaly is, in Keplerian motion the angle $\ell = nt + \ell_o$ where $n = 2\pi/P$ is the radial circular frequency. It will be very convenient in this Section to use units such as

$$G_N M_\odot = 1 \Rightarrow \mathcal{H}_o = -\frac{1}{2L^2}, \quad L = \sqrt{a}, \quad G = \sqrt{a(1 - e^2)}, \quad H = G \cos i. \quad (3.11)$$

The fact that the unperturbed Hamiltonian depends only on the action variable $L = I_r + I_\theta$, Eq. (3.4c), is the famous degeneracy of the Coulomb problem. [In quantum language, L corresponds to the principal quantum number $n_q = n_r + n_\theta = n_r + j$, while $G = J$ corresponds to j and, $H = J_z$ to m .] It implies immediately from the canonical equations (3.5) that the only fast angle variable is $\ell = nt + \ell_o +$ perturbations, where $n \equiv \partial\mathcal{H}_o/\partial L = L^{-3} = a^{-3/2}$. This is just Kepler's law, $n^2 a^3 = 1$, in our units where $G_N M_\odot = 1$.

We are interested in deriving the *secular* evolution of the elliptic elements a , e , i , or equivalently L , G , H , under the combined influence of the perturbations \mathcal{H}_1 and \mathcal{H}_p . This is simply obtained by averaging the canonical equations over the fast angles, i.e. all the mean anomalies of the problem: ℓ , ℓ_p . [We denote this average by an overbar.] By averaging Eqs. (3.5b) one sees easily that (in first order) L will be secularly constant (i.e. $a = \text{const}$), while G , H , g , h slowly evolve under the averaged perturbed Hamiltonian

$$\mathcal{H}_{\text{pert}}(L, G, H; g) = \overline{\mathcal{H}}_1(L, G) + \overline{\mathcal{H}}_p(L, G, H; g; L_p). \quad (3.12)$$

As already indicated in Eq. (3.12), the averaged perturbed Hamiltonian depends (besides $L = \sqrt{a}$ and $L_p = \sqrt{a_p}$ which can be treated as constants) only on G , H and $g = \omega$. We consider, for simplicity, that the planets move on circular orbits. The lack of dependence on the last angle $h = \Omega$ comes from the averaging over ℓ and ℓ_p which establishes an azimuthal symmetry in the averaged Hamiltonian. Because of this azimuthal symmetry, $dH/dt = -\partial\mathcal{H}_{\text{pert}}/\partial h = 0$, i.e. $H = J_z$ is a (secular) constant of the motion. Finally, we can treat L , H and L_p as constants, and consider only the evolution of the canonical pair $(G, g) = (J, \omega)$ under the Hamiltonian $\mathcal{H}_{\text{pert}}(G, g) = \overline{\mathcal{H}}_1(G) + \overline{\mathcal{H}}_p(G, g)$. But this is, in principle, a rather simple problem because we have now only one degree of freedom (one canonical pair), with a time-independent Hamiltonian. We conclude immediately that the perturbed energy is a constant of the motion. Therefore, it will be essentially enough to draw the phase-space picture of the problem via Hamiltonian level curves,

$$\mathcal{H}_{\text{pert}}(G, g) = \overline{\mathcal{H}}_1(G) + \overline{\mathcal{H}}_p(G, g) = E_{\text{pert}} = \text{const}, \quad (3.13)$$

to be able to control the secular evolution of G , i.e. of the angular momentum J . We must now compute explicitly the values of $\overline{\mathcal{H}}_1$ and $\overline{\mathcal{H}}_p$ to see when planetary perturbations can, via the equation $dG/dt = -\partial\mathcal{H}_{\text{pert}}/\partial g = -\partial\overline{\mathcal{H}}_p/\partial g$, force $G = J$ to evolve ultimately towards large enough values of J , corresponding to orbits which no longer traverse the Sun.

Let us first deal with the planetary perturbations. The calculation of $\overline{\mathcal{H}}_p$ over the WIMP phase space is, in principle, a complicated matter because the WIMP can sometimes have a near collision with a planet, especially with Venus which is as massive as the Earth and nearer to the Sun. [Remember that we are interested in a population of WIMPs with $a \sim 1$ AU, so that they can be detected on Earth.] In fact, we tried to estimate separately the effect of such near collisions on the evolution of $G = J$. They will cause G to undergo a kind of random walk, which can certainly help to increase G beyond $J_S = R_S v_{\text{esc}}(R_S)$. This effect is difficult to estimate with the kind of accuracy we attempt below for averaged perturbations, but it may be comparable to the effect we shall discuss below. By not including it explicitly, our estimate below of the fraction of WIMPs that can get kicked out of the Sun should thus be considered as a *lower bound*. To tackle analytically $\overline{\mathcal{H}}_p$ we shall assume that the WIMP orbit is sufficiently smaller than the planetary orbits considered to be able to expand \mathcal{H}_p in

powers of a/a_p and keep only the lowest significant (quadrupolar) contribution. [Actually, we have checked numerically that this quadrupolar approximation is surprisingly good even up to $a \simeq a_p/2$ for the very elliptic orbits we consider.] Doing the double average over ℓ and ℓ_p we find that the quadrupolar approximation to the second Eq. (3.9) (actually the last, dipolar, term averages to zero) yields

$$\begin{aligned}\overline{\mathcal{H}}_p &\simeq - \sum_p \frac{1}{2} \mu_p \langle x_X^i x_X^j \rangle_\ell \left\langle \partial_{ij} \frac{1}{|\mathbf{x}_p|} \right\rangle_{\ell_p} \\ &= - \sum_p \frac{\mu_p}{4 a_p^3} \langle r^2 - 3 z^2 \rangle_\ell.\end{aligned}\quad (3.14)$$

In terms of the *eccentric anomaly* u , we have [13]

$$\ell = u - e \sin u, \quad r = a(1 - e \cos u), \quad z = \sin i (\sin \omega \bar{x} + \cos \omega \bar{y}), \quad (3.15)$$

with (v denoting the true anomaly)

$$\bar{x} = r \cos v = a(\cos u - e), \quad \bar{y} = r \sin v = a \sqrt{1 - e^2} \sin u. \quad (3.16)$$

The average over ℓ is easily computed as a modulated average over u , namely for any quantity $q(\ell) = q(u)$

$$\langle q \rangle_\ell = \frac{1}{2\pi} \oint d\ell q = \frac{1}{2\pi} \oint du (1 - e \cos u) q = \langle (1 - e \cos u) q \rangle_u. \quad (3.17)$$

This yields

$$\left\langle \frac{r^2}{a^2} \right\rangle_\ell = 1 + \frac{3}{2} e^2, \quad \left\langle \frac{z^2}{a^2} \right\rangle_\ell = \frac{1}{2} \sin^2 i [1 + e^2 (4 - 5 \cos^2 \omega)], \quad (3.18)$$

so that

$$\overline{\mathcal{H}}_p = \sum_p -\frac{1}{4} \mu_p \frac{a^2}{a_p^3} \left[1 + \frac{3}{2} e^2 - \frac{3}{2} \sin^2 i - \frac{3}{2} e^2 \sin^2 i (5 \sin^2 \omega - 1) \right]. \quad (3.19)$$

To use this Hamiltonian in the canonical equations (3.5) one should think of all the elliptic elements a, e, i, ω as being expressed in terms of L, G, H, g . In particular, we recall that $L = \sqrt{a}$ and $H = G \cos i$ can be considered as constants, while $G = \sqrt{a(1 - e^2)}$ and $g \equiv \omega$ are the evolving variables. The dynamics resulting from the Hamiltonian $\overline{\mathcal{H}}_p(G, g)$, considered separately from $\overline{\mathcal{H}}_1(G, g)$, i.e. for orbits that stay outside the Sun, was studied some time ago by Kozai [14] (see also the works of the Russian school in Ref. [15], and Refs. [16,17] for studies in which this Hamiltonian is relevant). When considering the beginning of the evolution of G (while the WIMP is still in the outskirts of the Sun), it is essentially enough to use as Hamiltonian the g -dependent part of Eq. (3.19), i.e.

$$\overline{\mathcal{H}}_p^g = \sum_p + \frac{15}{8} \mu_p \frac{a^2}{a_p^3} e^2 \sin^2 i \sin^2 g, \quad (3.20)$$

with $e \approx 1$ (very elliptic orbits) and $i \approx \text{const}$ (because the fractional variation of the inclination while the WIMP is still in the Sun is small, being correlated through $H = G \cos i = \text{const}$ to the fractional variation of $G = J$). Indeed, the WIMP just migrates through an outer skin of the Sun).

Let us now consider the other perturbation, $\overline{\mathcal{H}}_1$, linked to the mass distribution in the Sun, Eq. (3.9). For this term, it is more convenient to write the ℓ -average in terms of an integral over the radial variable r (in terms of which $\delta U(r)$ is most easily expressed). To do that we can first replace the ℓ (or time) average by an average over the area measure $r^2 dv$ (Kepler's area law). Here, v is the true anomaly, so that the unperturbed trajectory on which we integrate is the ellipse $r = a(1 - e^2)/(1 + e \cos v)$. We can here replace $a(1 - e^2)$ by $J^2 = G^2$ (in our units) and replace e in the denominator (only) by one. [Indeed, we deal with very elliptical orbits with $1 - e^2 \sim R_S/a \ll 1$.] Differentiating the polar equation of the ellipse (approximated as a parabola) yields

$$r^2 dv \simeq \pm \frac{J r dr}{\sqrt{2r - J^2}}. \quad (3.21)$$

We then get

$$\overline{\mathcal{H}}_1 = -\frac{1}{\pi a^{3/2}} \int_{r_{\min}}^{r_{\max}} \frac{r dr}{\sqrt{2r - J^2}} \delta U(r) = -\frac{1}{2^{1/2} \pi a^{3/2}} \int_{r_{\min}}^{R_S} \frac{r dr}{\sqrt{r - r_{\min}}} \delta U(r). \quad (3.22)$$

Here, $r_{\min}(J)$ is the perihelion distance (closest radius) of the orbit such that $J^2 = 2r_{\min} \simeq (rv_{\text{esc}}(r))^2$, consistently with our definition of r_{\min} (for $J = J_{\min}$) in Section 2. [Indeed, $v_{\text{esc}}^2(r) \simeq 2G_N M_\odot/r$.] The maximum radius (which would be formally infinite for the parabolic approximation) plays no role because $\delta U(r)$ vanishes by definition outside the Sun.

To express explicitly $\overline{\mathcal{H}}_1$ in terms of r_{\min} (i.e. of $G \equiv J = \sqrt{2r_{\min}}$) we need to know the radial dependence of $\delta U(r)$ in the actual Sun. To do that we have fitted the radial mass distribution of the Sun, given numerically by Bahcall and Pinsonneault [18], to simple power laws. We find that the mass distribution in the outskirts of the Sun (we are interested in the last outer few percent of the mass of the Sun) is well approximated by the fit

$$\frac{\delta M(r)}{M_\odot} \equiv 1 - \frac{M(r)}{M_\odot} \simeq \epsilon_m \left[\left(\frac{\overline{R}_S}{r} \right)^3 - 1 \right]; \quad (r \gtrsim 0.55R_S), \quad (3.23)$$

where

$$\epsilon_m = 0.0219, \quad \overline{R}_S = 0.907 R_S. \quad (3.24)$$

When using this fit, one must use \overline{R}_S as an effective radius of the Sun beyond which the density vanishes (and $\delta U(r) = 0$). [This neglects only the outer 0.13 % mass of the actual Sun.] From the (effective) radial mass distribution (3.23) we can deduce both the density distribution ($\rho(r) \propto r^{-6} \Theta(\overline{R}_S - r)$) and (by integration of $dU(r)/dr = -G_N M(r)/r^2$) the Newtonian potential $U(r) = G_N M_\odot/r + \delta U(r)$. This gives

$$\delta U(r) = \epsilon_m \frac{G_N M_\odot}{\overline{R}_S} \left[\frac{\overline{R}_S}{r} - \frac{1}{4} \left(\frac{\overline{R}_S}{r} \right)^4 - \frac{3}{4} \right] \Theta(\overline{R}_S - r). \quad (3.25)$$

By inserting (3.25) into (3.22) we finally get

$$\overline{\mathcal{H}}_1(J) = \frac{\epsilon_m \overline{R}_S^{1/2}}{\pi 2^{1/2} a^{3/2}} h(x_{\min}), \quad x_{\min} \equiv \frac{r_{\min}}{\overline{R}_S} \equiv \frac{J^2}{2 \overline{R}_S}, \quad (3.26)$$

where we used $G_N M_\odot = 1$, and where we defined the dimensionless function

$$h(x_{\min}) \equiv \Theta(1 - x_{\min}) \int_{x_{\min}}^1 \frac{dx x}{\sqrt{x - x_{\min}}} \left[\frac{3}{4} + \frac{1}{4x^4} - \frac{1}{x} \right]. \quad (3.27)$$

It is important to realize that as $x_{\min} \rightarrow 1$, i.e. as we get out of the Sun, the (Hamiltonian) function $h(x_{\min})$ tends to zero as fast as

$$h(x_{\min}) \simeq \frac{8}{5} (1 - x_{\min})^{5/2} \Theta(1 - x_{\min}) \quad (3.28)$$

(because $\delta U(r)$ vanishes as $(r - \overline{R}_S)^2$). By contrast, we shall see below that the efficiency of the outer skin in orbit-capturing WIMPs vanishes only as $(1 - x_{\min})^{3/2}$. This difference in asymptotic decrease will help in getting more WIMPs out of the Sun.

As was explained above, the problem of selecting the values of the WIMP angular momentum $J \equiv G$ for which planetary perturbations are strong enough to kick the WIMPs out of the Sun can be reduced to studying the level curves of the Hamiltonian (using only the crucial g -dependent part of $\overline{\mathcal{H}}_p$, Eq. (3.20))

$$\mathcal{H}'_{\text{pert}} = \overline{\mathcal{H}}_1(G) + \overline{\mathcal{H}}_p^g(G, g) = \beta h\left(\frac{G^2}{2 \overline{R}_S}\right) + \alpha \sin^2 g, \quad (3.29)$$

where

$$\alpha = \frac{15}{8} a^2 \sin^2 i \sum_p \frac{\mu_p}{a_p^3}, \quad \beta = \frac{\epsilon_m}{\pi 2^{1/2}} \frac{\overline{R}_S^{1/2}}{a^{3/2}}. \quad (3.30)$$

Remember that the Hamiltonian function $h(x_{\min})$ (3.27) vanishes for $x_{\min} \geq 1$, i.e. when the angular momentum exceeds the value corresponding exactly to a grazing incidence, and behaves as $(8/5)(1 - x_{\min})^{5/2}$ when $x_{\min} \rightarrow 1^-$. The level curves of (3.29) for $x_{\min} < 1$ have the same shape as that of the Hamiltonian $\beta'(G - G_S)^2 + \alpha \sin^2 g$. This is nothing but a pendulum: $H_{\text{pend}} = \frac{1}{2} p_\theta^2 + \frac{1}{2} k \sin^2 \theta$. As is well known an essential element of the phase portrait of a pendulum is the *separatrix*, i.e. the level curve $H_{\text{pend}} = \frac{1}{2} k$ which passes through the unstable equilibrium position $p_\theta = 0$, $\theta = \pi/2 \bmod \pi$. This curve separates the oscillation motions (with θ oscillating, nonharmonically, around $\theta = 0 \bmod \pi$) from the libration ones (with θ changing monotonically, i.e. the pendulum going around in a sling motion). Similarly, in the case of the Hamiltonian (3.29) it is easy to see that the level curve $\mathcal{H}'_{\text{pert}} = \alpha$ (passing through $G^2 = 2 \overline{R}_S$, $g = \pi/2 \bmod \pi$), i.e.

$$h\left(\frac{G^2}{2 \overline{R}_S}\right) = \lambda_{a,i} \cos^2 g, \quad (3.31)$$

is a separatrix (for $G < G_S \equiv \sqrt{2 \overline{R}_S}$). Here

$$\lambda_{a,i} = \frac{\alpha}{\beta} = \lambda_1 \left(\frac{a}{a_1} \right)^{7/2} \sin^2 i, \quad a_1 \equiv 1 \text{ AU}, \quad (3.32a)$$

$$\lambda_1 = \frac{15}{8} \pi 2^{1/2} \frac{1}{\epsilon_m} \left(\frac{a_1}{R_S} \right)^{1/2} \sum_p \mu_p \left(\frac{a_1}{a_p} \right)^3. \quad (3.32b)$$

The separatrix (3.31) divides between: (i) the uninteresting (for us) *circulation* motions where the “momentum” $p_\theta \sim G - G_S$ keeps the same (negative) sign, i.e. the WIMP keeps traversing the Sun over and over again, and (ii) the *oscillation* (or *libration*) motions where the “momentum” $p_\theta \sim G - G_S$ starts with a negative value and evolves so as to reach the value zero (corresponding to a trajectory which exactly grazes the Sun) in a finite time. Beyond the boundary $G = G_S$ the Hamiltonian describing the evolution of the canonical pair (G, g) is the planetary perturbation $\overline{\mathcal{H}}_p(L, H; G, g)$ given by Eq. (3.19) in which one must replace

$$a = L^2, \quad e^2 = 1 - \frac{G^2}{L^2}, \quad \sin^2 i = 1 - \frac{H^2}{G^2}, \quad \omega \equiv g, \quad (3.33)$$

where L and H are treated as constants. The corresponding phase portrait is drawn in Figure 1. [This Figure displays the level curves of the more exact perturbation Hamiltonian (3.13), with $\overline{\mathcal{H}}_p(L, H; G, g)$ given by Eq. (3.19), instead of the approximate expression (3.20) used in the text.] The horizontal axis is the angle g (in radians), while the vertical axis is $\log_{10}(\widehat{G})$, where $\widehat{G} \equiv G/L = \sqrt{1 - e^2}$ denotes a “reduced” angular momentum. The numerical values used in Figure 1 are $a = 0.844a_1$, and an initial inclination $\cos^2(i_{\text{in}}) = 1/3$. The corresponding value for the Sun-grazing reduced angular momentum is $\widehat{G}_S = 0.1$. The separatrix discussed above lies in the domain $\widehat{G} < \widehat{G}_S$, i.e., $\log_{10}(\widehat{G}) < -1$, and defines the dividing line (not explicitly shown) between the trajectories that stay always below \widehat{G}_S and those which evolve towards larger \widehat{G} values. Note that, starting on the “initial surface” $G = G_S$, most trajectories (except a small neighbourhood of $g = 0 \text{ mod } \pi$) then evolve well away from the Sun to undergo large changes of \widehat{G} , up to values of order unity. In other words, once the very elliptic WIMP trajectory (initially with $\widehat{G}^2 = 1 - e^2 \sim 2R_S/a \sim \frac{1}{100}$) exits the Sun, it undergoes, under the planetary perturbations, a slow, secular evolution of its eccentricity and inclination, up to values $\widehat{G}^2 = 1 - e^2 \sim 1$ and corresponding high inclinations $i \sim \frac{\pi}{2}$, keeping $H/L = \sqrt{1 - e^2} \cos i$ constant.

We estimated the time scale for exiting the Sun, when starting on an initial “oscillation” trajectory with $G_{\text{in}} < G_S$. From the canonical equation $dG/dt = -\partial \mathcal{H}'_{\text{pert}}/\partial g$ and the constancy of $\mathcal{H}'_{\text{pert}}$, Eq. (3.29), the time it takes for G_{in} to evolve up to G_S is given by integrating

$$\frac{dt}{dG} = \mp (\alpha^2 - 4[\beta h(G/G_S) - c]^2)^{-1/2}, \quad (3.34)$$

where the constant c is related to the constant energy. By numerically integrating (3.34) over typical trajectories (not too near the separatrix on which it takes an infinite time to reach $G = G_S$) we found that it generically takes (for $a \sim 1$) less than 10^3 WIMP radial periods (i.e. less than 10^3 yr) for the eccentricity of the WIMP to increase sufficiently to exit the Sun. Then, when $G > G_S$ the time scale for the evolution of G is given by the planetary

perturbations alone and is roughly $[\sum_p \mu_p (a/a_p)^3]^{-1}$ longer than one orbital period, i.e. roughly 10^5 yr for $a \sim a_1 \equiv 1$ AU. After this time, the WIMP would, if it evolved only under the simplified planetary Hamiltonian $\overline{\mathcal{H}}_p$, come back again to low values of G , corresponding to Sun-penetrating orbits. Under the influence of $\overline{\mathcal{H}}_1$, it would then again bounce back away from the Sun in $\sim 10^3$ orbits. For the scattering cross sections we shall be discussing below, the opacity of the small outer skin of the Sun we are interested in is typically smaller than $\sim 10^{-6}$. Therefore the above process could persist for thousands of cycles before the WIMP gets scattered by a nucleus in the outskirts of the Sun. However, as we mentioned earlier, it is clear that the real gravitational interaction of the WIMP with planets is much more complicated than what is described by $\overline{\mathcal{H}}_p$. In particular, the non zero eccentricities of the planets, and the occurrence, once in a while, of a near collision with an inner planet will cause the elliptic elements of the WIMP to diffuse chaotically away from the simplified periodic history described above. Moreover, the very high eccentricities (for AU-size orbits) needed to traverse again the Sun represent only a very small fraction of the phase space into which the WIMP can diffuse. It thus seems clear that on time scales of several million years most of the population of WIMPs we are talking about will have irreversibly evolved onto trajectories on which the WIMP can survive (without being scattered again in the Sun) for the age of the solar system. We will come back later to the problem of the long-term survival of such WIMPs on orbits that stay within the inner solar system (rather than diffusing out into the outer solar system, and eventually to infinity).

IV. ESTIMATING THE CAPTURE RATE OF LONG-SURVIVING, SOLAR-SYSTEM BOUND WIMPS

In view of the previous estimates and arguments, we can consider that the population of WIMPs that, after a first scattering event in the Sun, diffuse out onto long-surviving solar-bound orbits is given by all the initial conditions $G_{\text{in}}, g_{\text{in}}, i_{\text{in}}$ which are “above” the separatrix (3.31) (meaning $G_{\text{separatrix}} < G < G_S$). The logic for quantitatively estimating that population is the following. For each given initial values of a, g_{in} and i_{in} , the separatrix defines, by solving Eq. (3.31) with respect to G , a corresponding minimum value of G

$$J_{\text{min}} \equiv G_{\text{min}} = G_{\text{separatrix}}(a, g_{\text{in}}, i_{\text{in}}), \quad (4.1)$$

such that the trajectories with $J > J_{\text{min}}$ end up out of the Sun. The differential capture rate corresponding to this class $J > J_{\text{min}}$ is then precisely defined by our previous result (2.22) which defines

$$\frac{d\dot{N}_A}{d\alpha} = \mathcal{C}_A [J_{\text{min}}(a, g_{\text{in}}, i_{\text{in}}), \alpha]. \quad (4.2)$$

Then the actual capture rate is obtained by averaging (4.2) over the distribution of initial values $g_{\text{in}}, i_{\text{in}}$.

Let us first approximate the result (2.22) by a simpler expression. In the radial integration of Eq. (2.22) the crucial features are the radial dependence of the abundance of element A , $n_A(r)$, and the square root factor which vanishes at $r = r_{\text{min}}$. By contrast, the function $K_A(r, \alpha)$, Eq. (2.27), varies fractionally very little over the small integration range $\overline{R}_S(1-\epsilon) <$

$r < \bar{R}_S$ we are interested in. Therefore a good approximation of Eq. (2.22) consists of taking out in front a factor $K_A(\bar{R}_S, \alpha)$ and performing the radial integration on the remaining r -dependent factors. To do that let us consider again the r -dependence of the total mass of the Sun. Denoting $\mu(r) \equiv M(r)/M_\odot$, with $0 \leq \mu(r) \leq 1$, we have from Eq. (2.26)

$$d\mu(r) = 3 \epsilon_m \frac{\bar{R}_S^3 dr}{r^4} = 3 \epsilon_m \frac{dx}{x^4}, \quad (4.3)$$

where ϵ_m was given in Eq. (3.24) and where $x \equiv r/\bar{R}_S$. The distribution of the density of element A can be written as

$$d^3 \mathbf{x} n_A(\mathbf{x}) = 4\pi r^2 dr n_A(r) = f_A \frac{M_\odot}{m_A} d\mu(r), \quad (4.4)$$

where f_A denotes the mass fraction of element A in the outskirts of the Sun. Let us define the following (“capture”) function

$$c(x_{\min}) \equiv \int_{x_{\min}}^1 \frac{dx}{x^4} \sqrt{1 - \frac{x_{\min}}{x}} = \int_{x_{\min}}^1 \frac{dx(x - x_{\min})^{1/2}}{x^{9/2}}. \quad (4.5)$$

In terms of this capture function, the capture rate reads

$$\left. \frac{d\dot{N}_A}{d\alpha} \right|_{J_{\min}} = \frac{n_X}{v_o} f_A \frac{M_\odot}{m_A} \sigma_A K_A^s(\alpha) 3 \epsilon_m c(x_{\min}), \quad (4.6)$$

where K_A^s is the “surface” value of the radial function explicitly defined in Eq. (2.27)

$$K_A^s(\alpha) \equiv K_A(\bar{R}_S, \alpha). \quad (4.7)$$

Note that the surface value of the quantity $A(r)$ entering the error functions in (2.27) is

$$(A(\bar{R}_S))^2 \equiv (1 + \hat{a}_A) \frac{\beta_-^A}{v_o^2} \left(\bar{v}_S^2 - \frac{\alpha}{\beta_+^A} \right), \quad \bar{v}_S^2 = G_N M_\odot / \bar{R}_S = (648.3 \text{ km/s})^2. \quad (4.8)$$

Actually, as said above, the α -dependence of K_A^s is negligible (especially in view of all our other approximations) because $\alpha \sim v_E^2 \sim (30 \text{ km/s})^2$ so that $\bar{v}_S^2/\alpha \sim 467 \gg 1$. Therefore the α -dependence of $d\dot{N}_A/d\alpha|_{J_{\min}}$ will come from the a -dependence of the “ejectable” radius x_{\min} , to the estimate of which we now turn.

Both the “capture function” $c(x_{\min})$ and the previously introduced “hamiltonian function” $h(x_{\min})$, Eq. (3.27), can be explicitly expressed in terms of elementary functions. But these explicit expressions will not be really needed here. On the other hand, it is important to note the asymptotic behaviour of $c(x_{\min})$ as $x_{\min} \rightarrow 1^-$:

$$c(x_{\min}) \simeq \frac{2}{3} (1 - x_{\min})^{3/2}. \quad (4.9)$$

The fact that $c(x_{\min}) \propto (1 - x_{\min})^{3/2}$ decreases less fast than $h(x_{\min}) \propto (1 - x_{\min})^{5/2}$, Eq. (3.28), as $x_{\min} \rightarrow 1^-$ is important for us because the width of the separatrix (3.31), $h(x_{\min}) = \mathcal{O}(\lambda_{a,i})$, will be converted in a capture rate proportional to $\lambda_{a,i}^{3/5}$, i.e. something

larger than the *a priori* expected small perturbation parameter $\lambda_{a,i} = \alpha/\beta \propto \mu_p/a_p^3$. If we were to use only the asymptotic expressions (3.28), (4.9) the width of the separatrix (3.31) would be $1 - x_{\min} \simeq (5 \lambda_1/8)^{2/5} (a/a_1)^{7/5} (\sin i)^{4/5} (\cos g)^{4/5}$, and the corresponding capture rate would be proportional to

$$c_{\text{asymptotic}}(x_{\min}) \simeq \frac{2}{3} \left(\frac{5 \lambda_1}{8} \right)^{3/5} \left(\frac{a}{a_1} \right)^{\frac{21}{10}} (\sin i)^{6/5} (\cos g)^{6/5}. \quad (4.10)$$

The actual capture rate will be larger than the one predicted by (4.10) because the actual function $c(x_{\min})$ increases faster than (4.9) as one gets into the Sun. To combine some adequate numerical accuracy with the convenience of having analytical expressions we shall assume the approximate validity of the scalings in a/a_1 , $\sin i$ and $\sin g$ predicted by Eq. (4.10) but calculate the precise numerical coefficient applicable for $a/a_1 = \sin i = \cos g = 1$ by using the full numerical expressions of the functions $h(x)$ and $c(x)$, i.e. by inverting $h(x_1) = \lambda_1$ in x_1 and computing $c(x_1)$. To do this we need the numerical value of λ_1 . First, taking into account the most significant planets, i.e. Venus, the Earth, Mars, Jupiter and Saturn, we find

$$\sum_p \mu_p \left(\frac{a_1}{a_p} \right)^3 = 1.67 \times 10^{-5}, \quad (4.11)$$

where we recall that a_1 denotes simply the basic unit for semi-major axes, namely the astronomical unit (AU). The other important numerical ingredients in λ_1 , Eq. (3.32b), are

$$\left(\frac{a_1}{R_S} \right)^{1/2} = (236.9)^{1/2} = 15.39, \quad \epsilon_m = 0.0219, \quad (4.12)$$

so that

$$\lambda_1 = 0.0978. \quad (4.13)$$

The corresponding solution of $h(x_1) = \lambda_1$ is $x_1 = 0.729$ (which means that we are typically dealing with the outer 27 % of the Sun radius-wise, containing in fact only ~ 2 % of the mass of the Sun). The corresponding value of the capture function is $c(x_1) = 0.172$, so that the numerical combination effectively appearing in the capture rate (4.6) will equal (when $a/a_1 = \sin i = \cos g = 1$)

$$3 \epsilon_m c(x_1) = 0.0113. \quad (4.14)$$

This value must, according to Eq. (4.10), be scaled by $(a/a_1)^{2.1} (\sin i)^{6/5} (\cos g)^{6/5}$. Here, i and g are the initial values of the inclinations and perihelion argument. These quantities are random variables: g is expected to have a uniform distribution over $[0, 2\pi]$, while it is $\cos i$ which is expected to have a uniform distribution over $[0, 1]$ (indeed, the direction of the vectorial angular momentum \mathbf{J} is expected to be random on the celestial sphere). The averaging over these variables brings a factor

$$\langle (\sin i)^{6/5} \rangle_{\cos i} \langle (\cos g)^{6/5} \rangle_g = 0.7567 \times 0.6007 = 0.4545. \quad (4.15)$$

Together with (4.14) and the a -scaling we end up with a fraction kicked out of the Sun,

$$\phi(a) \equiv 3 \epsilon_m \langle c(x_{\min}) \rangle \simeq \phi_1 \left(\frac{a}{a_1} \right)^{\frac{21}{10}}, \quad \phi_1 \simeq 5.13 \times 10^{-3}. \quad (4.16)$$

Finally, if we define the A -dependent combination

$$g_A \equiv \frac{f_A}{m_A} \sigma_A K_A^s, \quad (4.17)$$

the rate (per $\alpha = G_N M_\odot/a$) of solar capture of WIMPs that subsequently survive out of the Sun to stay within the inner solar system, reads

$$\left. \frac{d \dot{N}_A}{d \alpha} \right|_{\text{surv}} = \phi_1 \left(\frac{a}{a_1} \right)^{\frac{21}{10}} M_\odot \frac{n_X}{v_o} g_A. \quad (4.18)$$

Note that the A -dependence is entirely contained in the quantity g_A with dimensions [cross section]/[mass], e.g. [cm²]/[GeV/ c^2], or GeV⁻³ in particle units. The total capture rate is given by $\sum_A g_A$.

V. ESTIMATING THE PRESENT LOCAL PHASE-SPACE DISTRIBUTION OF SURVIVING SOLAR-CAPTURED WIMPS

The last result (4.18) of the previous Section gives the rate with which a fraction of the WIMP-Sun-scattering events populates a class of WIMPs that get out of the Sun with initial semi-major axis equal to a , and very high initial eccentricities such that

$$1 - e^2 = 2 \frac{\overline{R}_S}{a} \simeq 8.44 \times 10^{-3} \frac{a_1}{a}. \quad (5.1)$$

The question that remains is the following: what happens to this population while it slowly builds up during the 4.5 Gyr lifetime of the solar system? What is the present local distribution (in position and velocity space) as seen from the Earth of these WIMPs? These questions are very difficult to answer with precision because of the complexity of Hamiltonian dynamics in the solar system. One would need long-term numerical simulations to give reliable quantitative answers. However, we shall attempt here to make some estimates that will allow us to estimate the present observable effects of this population of WIMPs.

There are two main worries about the long-term survival of this population. The first would be that they traverse the Sun again and again and end up getting accreted by it. We argued away this worry above (because of the very small opacity of the outer skin of the Sun, of the repelling effect of the interaction with $\delta U(r)$, and of the small probability, given some additional chaos, that the WIMP again encounters the Sun). Note that existing asteroid simulations (see e.g. [19]) do not help in this respect because: (i) they restrict themselves to essentially planar initial data (while our WIMPs have fully three-dimensional trajectories), and (ii) they stop their numerical integrations as soon as an asteroid touches the Sun (while our WIMPs could survive $\sim 10^5 - 10^6$ passes in the outskirts of the Sun).

[Note that, in the case of the “lowest” ($a = 2.1\text{AU}$) orbits considered in [19], 79% of them were eliminated because of impacting on the Sun.] A second worry concerns the possibility that the adiabatic invariant a slowly evolves, in a quasi-random-walk, under the effect of near collisions with planets. This diffusion in a -space could lead a fraction of the WIMPs to have higher and higher values of a , possibly being ejected from the solar system. One can give a crude analytical estimate of the time scale on which a can change in the following way. Because of the exponential accuracy with which adiabatic invariants are conserved in absence of near collisions (i.e. in absence of near singularities in the complex plane, see e.g. [11]), the cause of the random walk of a must be the existence of near collisions with some planet. Therefore, this effect will depend very much on the value of a . If a is smaller than $a_J/2 \simeq 2.6 a_1$ (where the label J stands for Jupiter) the WIMP orbit cannot cross Jupiter’s orbit even if the eccentricity is very high. In that case, only one of the inner planets can have a near collision with a WIMP. Let generally m_p be the mass of a planet whose orbit can cross that of a WIMP, with semi-major axis a_X . The only small parameter in the problem of the non adiabatic evolution of a_X is $\mu_p \equiv m_p/M_\odot$ (we use units such that $G_N M_\odot = 1$). This non adiabatic evolution will be due to a more or less random succession of near collisions with the planet. Each collision would induce a velocity change $\delta v \sim \mu_p/(bv)$ and an energy change $\delta a_X/a_X \sim \pm \mu_p a_X/b$ where b is the impact parameter. The rate of occurrence of such collisions is smaller as b decreases. Between two such quasi-collisions all the angular variables in the problem (which determine the \pm sign in the energy change) have probably had the chance of being essentially randomized. After a long time t we can then consider that the total fractional change of a_X , Δa_X , is a random walk so that one must consider $(\Delta a_X/a_X)^2 \sim \sum_{\text{collisions}} (\mu_p a_X/b)^2$. If we provisionally use units where $a_X = 1$, one can see that the typical time between two near collisions with impact parameter b is $t_b \sim b^{-2}$ (b^2 is an effective cross section around the planet, while the WIMP is evolving in a full $3D$ -volume $\sim a_X^3 = 1$). The number of terms in the above random-walk is then $N \sim t/t_b \sim b^2 t$ so that $(\Delta a_X)^2 \sim N (\mu_p/b)^2 \sim \mu_p^2 t$. Returning to ordinary units we find a typical diffusion law

$$\left(\frac{\Delta a_X}{a_X}\right)^2 \sim \frac{t}{t_D}, \quad t_D = C \mu_p^{-2} T_X, \quad (5.2)$$

where T_X is the orbital period corresponding to a_X , and where C is some numerical constant of order unity. The dimensionless constant C is impossible to estimate with any accuracy on the basis of the previous rough argument (it can also contain a logarithm due to the integration over a relevant range of values of b). The estimate (5.2) suggests that the semi-major axis of Earth-crossing WIMPs diffuse on a very long time scale $t_D \sim C (3.3 \times 10^5)^2 (a_X/a_1)^{3/2} \text{yr} \sim C \times 10^{11} (a_X/a_1)^{3/2} \text{yr}$, so that we can essentially neglect the variation of a_X over the age of the Sun. By contrast, the situation becomes dramatically different when $a_X = a_J/2 = 2.6 a_1$, because in this case it can cross the orbit of Jupiter with $\mu_p \simeq (1047)^{-1}$. This leads to a much shorter diffusion time scale $t_D^J \sim 4.6 \times C \times 10^6 (2 a_X/a_J)^{3/2} \text{yr}$. The existence of such very different time scales depending on $a_X < a_J/2$ or $a_X > a_J/2$ is well known in asteroid research and is apparent in the results of long-term numerical simulations, see, e.g., Ref. [20]. In principle such numerical simulations can give estimates of the diffusion times. It seems that a value of $C \sim 0.1$ is roughly compatible with several results and numbers in the literature [20], [21], though the comparison might be difficult because asteroid

simulations start with quasi-planar initial conditions.

To summarize: we expect, in first approximation, that the initial a -distribution derived in previous Sections can build up over $t_S = 4.5$ Gyr with only small diffusion effects if $a < a_J/2 = 2.6 a_1$, while if $a > a_J/2$ this population is cut-off because of a fast diffusion in the outskirts of the solar system. As we said above, this conclusion, based on our analytical estimate Eq. (5.2), should be checked by dedicated long-term numerical simulations.

Having discussed the secular evolution of a , we need now to discuss that of e and the other elliptic elements. As shown in Eq. (5.1) the initial values of the eccentricities are very near 1. The discussion of the phase portrait of the secular planetary Hamiltonian $\overline{\mathcal{H}}_p$ in Section III showed that e and i undergo large oscillations with e evolving between values very near 1 and values of order one (say 0.3). The lower values of e depend on the value of $H = J_z = \sqrt{a(1 - e^2)} \cos i$ which is a secular invariant. Note that we now consider the dynamics implied by the Hamiltonian $\overline{\mathcal{H}}_p$, without the solar contribution $\overline{\mathcal{H}}_1$. The phase portrait of $\overline{\mathcal{H}}_p$ differs from Fig. 1 in that the level curves escaping from the Sun and formerly librating around $g = 0$ or π , are now circulating, i.e. such that the angle g is monotonically evolving. The phase portrait of this pure Kozai Hamiltonian is represented, for instance, in [14] (Fig. 8), or [17] (Fig. 3). For our case (a very small value of the constant of motion H/L) this means that most orbits will feature a small value of G/L , i.e. a large value of the eccentricity e , for a wide range of values of the periastron argument g (a maximal eccentricity is reached for $g = \pi/2$ or $3\pi/2$, but this maximum is broad, and large eccentricities are maintained during most of the evolution).

In addition, the time-averaged probability for the eccentricity to fall in the range $e \pm \frac{1}{2} de$, will be peaked toward the extremal values of $e(t)$ (because $dt = de/\dot{e}$ diverges there). The maximal value of e is very near 1 for all the WIMPs of the population, while the minimal value varies across the WIMP population, because it depends, among other initial data, on the value of the constant of motion $H = \sqrt{a(1 - e^2)} \cos i$. Therefore the overall time-averaged and population-averaged distribution function for e will have a peak only near $e \approx 1$. But, as we said above, this peak should be superposed onto a rather flat distribution favoring high values of the eccentricity. (Therefore the fact that the maximal eccentricities of each orbit are reached for $g = \pi/2$ or $3\pi/2$, which implies a lack of spherical symmetry of the spatial distribution of the WIMPs, and which thereby somewhat disfavors the ecliptic plane, should not be numerically very significant). In the absence of detailed numerical simulations of the long-term evolution of our population of WIMPs this argument (based on the simplified secular Hamiltonian (3.19)) suggests to use as an educated guess, for the mean distribution function of e , a distribution peaked at $e = 1$, i.e. simply a delta function $\delta(1 - e)$. Numerical simulations of asteroids, which go beyond the simplified Hamiltonian (3.19) and take into account near collisions with the planets, suggest that the analytically-expected large oscillations in e may actually be damped and lead to a population always having quite large eccentricities (see Fig. 4 in Ref. [20]). Resolving this question, and investigating the actual deviation from spherical symmetry of the WIMP population, would demand the running of long-term numerical simulations. In the present paper, we shall assume, for illustration purposes, a spherically symmetric population formally entirely concentrated at $e \approx 1$, which is technically simpler to deal with than a more realistic range of high values of e . Certainly, some of the details of the predictions that we shall sketch below depend on

this assumption, but we think that it is an appropriate approximation at this stage, though one which will have to be checked by dedicated numerical simulations.

Under this assumption we can compute both the present space distribution and the present velocity distribution of our population of WIMPs. Let us first consider the spatial (numerical) density of WIMPs $n(r)$. Consider first a subpopulation with some given values of a and e . By differentiating $r = a(1 - e \cos u)$, $\ell = u - e \sin u$ we find

$$d\ell/dr = \pm a^{-2} r (e^2 - (1 - r/a)^2)^{-1/2} \quad (5.3)$$

so that the fraction of time, or elementary probability $dp = 2|d\ell/dr| dr/2\pi$ (where the extra factor 2 comes from the sign ambiguity), spent by this subpopulation within the radii r and $r + dr$ is

$$dp = \frac{1}{\pi a^2} \frac{r dr}{\sqrt{e^2 - (1 - r/a)^2}} \Theta(r - a(1 - e)) \Theta(a(1 + e) - r). \quad (5.4)$$

From our previous arguments the number of WIMPs with semi-major axis within $[a, a + da]$ is

$$\frac{dN}{da} da = \frac{dN}{d\alpha} d\alpha = t_S \frac{d\dot{N}}{d\alpha} d\alpha, \quad (5.5)$$

where $t_S \simeq 4.5$ Gyr is the age of the Sun, and where, from Eq. (4.18)

$$\frac{d\dot{N}}{d\alpha} = \Theta\left(\frac{1}{2}a_J - a\right) \phi_1\left(\frac{a}{a_1}\right)^{2.1} M_\odot \frac{n_X}{v_o} g_{\text{tot}}, \quad g_{\text{tot}} = \sum_A g_A. \quad (5.6)$$

The average number of WIMPs within the radii $r, r + dr$ is obtained by multiplying (5.4) and (5.5) and integrating over a ,

$$d_r N = 4\pi r^2 dr n(r) = \int da \frac{dN}{da} dp, \quad (5.7)$$

so that the density of WIMPs reads (using $|d\alpha| = G_N M_\odot da/a^2$)

$$n(r) = \frac{1}{4\pi^2 r} \int da \frac{G_N M_\odot}{a^2} t_S \frac{d\dot{N}}{d\alpha} \frac{\Theta(r - a(1 - e)) \Theta(a(1 + e) - r)}{a^2 \sqrt{e^2 - (1 - r/a)^2}}. \quad (5.8)$$

If we were to consider a population distributed in eccentricity with weight $\varphi(e) de$, we would need to add a further integration $\int de \varphi(e)$ in front of Eq. (5.8). Here, as we have mentioned, we shall simply assume that $e \approx 1$ for the entire population. It is then convenient to replace a by the new integration variable $x \equiv 2a/r$. Inserting Eq. (5.6) in Eq. (5.8) and remembering the various step functions that limit the a -integration range we get

$$n(r) = \nu_1 n_X \left(\frac{a_1}{r}\right)^{1.9} I_n\left(\frac{a_J}{r}\right), \quad (5.9)$$

where

$$\nu_1 = \frac{\phi_1}{2^{2.1} \pi^2} t_S \frac{G_N M_\odot}{a_1^4} \frac{M_\odot g_{\text{tot}}}{v_o}, \quad (5.10)$$

$$I_n(y) \equiv \int_1^y \frac{dx}{x^{0.9} \sqrt{x-1}}. \quad (5.11)$$

As $I_n(a_J/r)$ tends to a finite limit as $r \ll a_J$, we see that the radial dependence of the WIMP density is essentially given by the factor $(a_1/r)^{1.9}$. This indicates that, if it were possible to do so, it would be easier to detect the WIMP population we are talking about nearer to the Sun, e.g. by building a detector in a mine (or examining WIMP-induced tracks in ancient mica) on Mercury! Let us also note that the radial distribution $n(r)$ probably becomes cut off below some radius $r_c < a_M = 0.387 a_1$, M being a label for Mercury. Indeed, for $a_X < a_M/2$ WIMPs do not have near collisions with any of the planets. Their secular orbital evolution should be rather well described by the quadrupolar Hamiltonian $\overline{\mathcal{H}}_p$, which means that they will episodically but repeatedly penetrate the outskirts of the Sun, thereby risking more to be scattered again. There should exist a critical semi-major axis a_c , between \overline{R}_S and $a_M/2$, such that when $a_X < a_c$ the WIMP penetrates the Sun too often and finally gets accreted.

In the following we shall focus on the value of the density of WIMPs at the orbital radius of the Earth, $r_E = a_1 \equiv 1 \text{ AU}$. Let us define the enhancement in WIMP density due to the secondary population considered here as

$$\delta_E \equiv \frac{n(a_1)}{n_X} \equiv \frac{\text{(secondary) WIMP density at the Earth}}{\text{halo WIMP density at infinity}}. \quad (5.12)$$

From Eqs. (5.9), (5.10) one finds

$$\delta_E = \phi_2 \Delta g_{\text{tot}}, \quad (5.13)$$

with (using $G_N M_\odot/a_1 = v_E^2$ with $v_E = 29.78 \text{ km/s}$, and $I_n(5.2) = 2.3474$)

$$\phi_2 = \phi_1 \frac{I_n(5.2)}{2^{2.1} \pi^2} = \phi_1 \times 0.0555 = 2.85 \times 10^{-4}, \quad (5.14)$$

$$\Delta = \frac{v_E^2}{v_o} t_S \frac{M_\odot}{a_1^3} = \frac{1.91 \times 10^{40}}{(v_o/220 \text{ kms}^{-1})} \text{ GeV cm}^{-2} = \frac{7.44 \times 10^{12}}{(v_o/220 \text{ kms}^{-1})} (\text{GeV})^3. \quad (5.15)$$

Finally the local enhancement in density is

$$\delta_E = \frac{5.44 \times 10^{36}}{(v_o/220 \text{ kms}^{-1})} \times g_{\text{tot}} \text{ GeV cm}^{-2} = \frac{0.212}{(v_o/220 \text{ kms}^{-1})} g_{\text{tot}}^{(-10)}, \quad (5.16)$$

where $g_{\text{tot}}^{(-10)} \equiv 10^{10} g_{\text{tot}} (\text{GeV})^3$. The meaning of the $10^{10} (\text{GeV})^3$ factor is that in $g_{\text{tot}} = \sum_A (f_A/m_A) \sigma_A K_A^s$, with dimensions $[\text{mass}]^{-1} \times [\text{cross section}]$, one must express the mass in units of GeV and the cross section in units of $10^{-10} \text{ GeV}^{-2}$ (with $\hbar = c = 1$). Note the conversion factor $\text{GeV}^{-2} = 3.8938 \times 10^{-28} \text{ cm}^2$. We shall see in the next Section that $g_{\text{tot}}^{(-10)}$ can be higher than ~ 1 , so that this new population could represent a significant increase above the standard halo WIMP density.

VI. OBSERVABLE SIGNALS FROM THE NEW WIMP POPULATION

The secondary WIMP population discussed here could give rise to observationally significant effects that have not traditionally been taken into account in the standard approach to dark matter detection, where one considers only the primary galactic halo population. The main observable signals from the new population are: (i) a new component, involving \sim keV energy transfer, in the differential spectrum of direct detectors of WIMPs, (ii) a significantly different angular spectrum in any detector with directional sensitivity, and (iii) a possible significant increase in the indirect neutrino signal caused by WIMP annihilations in the Earth. To discuss the figures of merit associated with the new WIMP population, we need to fold in the velocity distribution of the WIMPs. Eq. (5.3) above, together with $d\ell/dt = n = (G_N M_\odot/a^3)^{1/2}$, shows that the radial velocity $v_r = dr/dt$ of a WIMP passing at radius r reads

$$v_r = \pm \frac{1}{r} \left(\frac{G_N M_\odot}{a} \right)^{1/2} (e^2 a^2 - (a-r)^2)^{1/2}. \quad (6.1)$$

The local velocity of a WIMP in the Earth frame is $\mathbf{v}_{\text{loc}} = \mathbf{v}_X - \mathbf{v}_E$, where \mathbf{v}_X is the heliocentric WIMP velocity, whose radial component is (6.1). In our approximation where $e \approx 1$ for all the WIMPs \mathbf{v}_X is in the radial direction (with $|\mathbf{v}_X| = |v_r|$), and therefore orthogonal to the Earth orbital velocity \mathbf{v}_E . This yields $v_{\text{loc}}^2 = v_r^2 + v_E^2$ so that, with $r = a_1 = 1 \text{ AU}$,

$$v_{\text{loc}} = v_E \left(3 - \frac{a_1}{a} \right)^{\frac{1}{2}}. \quad (6.2)$$

With $a_1/2 \leq a \leq a_J/2 = 2.6 a_1$, this predicts that the local velocity of the secondary WIMPs we discuss ranges only between $v_E = 29.8 \text{ km/s}$ and $\sqrt{3 - 1/2.6} v_E = 48.2 \text{ km/s}$. These numbers depend on our approximation $e \approx 1$. They are, however, indicative of the values we might expect for the actual population. The local distribution is obtained by eliminating a using (5.5) and (6.2).

Actually, the observable of most interest is the differential rate (events per kg per day and per keV) of scattering events in a laboratory sample made of element A [5]

$$\frac{dR}{dQ} = \frac{\sigma_A n}{2 m_{\text{red}}^2(X, A)} F_A^2(Q) \int_{v_{\text{min}}(Q)}^{\infty} \frac{d\hat{n}(v)}{v}, \quad v_{\text{min}}(Q) = \left(\frac{Q m_A}{2 m_{\text{red}}^2(X, A)} \right)^{1/2}. \quad (6.3)$$

Here, $Q = \mathbf{q}^2/(2 m_A) = (m_{\text{red}}^2/m_A) v_{\text{loc}}^2 (1 - \cos \theta_{\text{cm}})$ is the energy transfer from the WIMP X to the nucleus A , $m_{\text{red}}(X, A) \equiv m_X m_A/(m_X + m_A)$ is the reduced mass, n is the local number density of the considered WIMP population, F_A^2 the form factor (2.7), v the local WIMP velocity and $d\hat{n}(v)$ the *normalized* speed distribution of the WIMP number density, with $\int d\hat{n}(v) = 1$. Note that for the standard WIMP population $n^{\text{standard}} = n_X$, while for the new population discussed here $n^{\text{new}} = \delta_E n_X$. Following Ref. [5], one can introduce for any WIMP population the dimensionless quantity

$$T(Q) = \frac{\sqrt{\pi}}{2} v_o \int_{v_{\text{min}}(Q)}^{\infty} \frac{d\hat{n}(v)}{v}. \quad (6.4)$$

For the standard galactic halo WIMPs

$$T_{\text{standard}}(Q) \simeq \exp(-v_{\text{min}}^2/v_o^2) = \exp\left(-\frac{m_A Q}{2v_o^2 m_{\text{red}}^2}\right), \quad (6.5)$$

when neglecting the motion of the Earth with respect to the halo. For the low velocity WIMPs we are considering $T_{\text{standard}}(Q) \simeq 1$. Therefore the ratio

$$\rho(Q) \equiv \frac{(dR/dQ)^{\text{new}}}{(dR/dQ)^{\text{standard}}} \equiv \delta_E \frac{T^{\text{new}}(Q)}{T^{\text{standard}}(Q)} \simeq \delta_E T^{\text{new}}(Q). \quad (6.6)$$

This quantity is the figure of merit of most interest to us. It expresses the fractional increase, with respect to standard expectations, in the differential scattering rate. The distribution $\frac{d\hat{n}^{\text{new}}}{da} da$ is obtained by taking the integrand of Eq. (5.8) and normalizing it to one. Changing the integration variable from a to $x = 2a/r = 2a/a_1$ gives

$$d\hat{n} = \frac{1}{I_n(5.2)} \frac{dx \Theta(x-1) \Theta(5.2-x)}{x^{0.9} \sqrt{x-1}}. \quad (6.7)$$

One must then bring in the factor $1/v = 1/(v_E \sqrt{3-2x^{-1}})$ from Eq. (6.2). Let us define the energy scale

$$Q_E \equiv 2 \frac{m_{\text{red}}^2}{m_A} v_E^2 = 2 \left(\frac{m_X}{m_X + m_A} \right)^2 m_A v_E^2. \quad (6.8)$$

For natural Germanium $\langle m_A \rangle \simeq 73 \text{ GeV}$ this scale is $Q_E \simeq 1.5 (m_X/(m_X + m_A))^2 \text{ keV}$. Let us also define the function

$$D(q) \equiv \frac{1}{I_n(5.2)} \int_{x_{\text{min}}(q)}^{5.2} dx \frac{\Theta(x-1)}{x^{0.9} \sqrt{x-1} \sqrt{3-2x^{-1}}}, \quad x_{\text{min}}(q) \equiv \frac{2}{3-q}, \quad (6.9)$$

where $I_n(5.2) = 2.3474$ is the integral (5.11). In terms of these definitions, the figure of merit (6.6) reads

$$\rho(Q) = \rho_1 D\left(\frac{Q}{Q_E}\right), \quad (6.10a)$$

$$\rho_1 = \frac{\sqrt{\pi}}{2} \frac{v_o}{v_E} \delta_E = 1.39 g_{\text{tot}}^{(-10)}. \quad (6.10b)$$

The function $D(q)$, with $q \equiv Q/Q_E$ is plotted in Figure 2.

The plateau that is reached by $D(q)$ as soon as $q \leq 1$ (i.e. $Q \leq Q_E$) has value $D(1) = 0.803$. This gives the maximal figure of merit [7]

$$\rho(Q_E) = 1.11 g_{\text{tot}}^{(-10)}. \quad (6.11)$$

If $g_{\text{tot}}^{(-10)} \sim 1$ (see below), this yields a 100 % increase of the differential event rate below $Q = Q_E \sim \text{keV}$.

Also, within our present rough approximation, $e \approx 1$, the direction of the incoming WIMPs from the new population will be *strongly anisotropic*. Indeed, not only are they entirely confined in the ecliptic plane, but even in this plane they have velocities whose local direction is within $\pm \tan^{-1} \sqrt{2(1 - 1/5.2)} = \pm 51.8^\circ$ of the vector $-\mathbf{v}_E$. This directional information might greatly help in distinguishing the real events from the background if one had a directional detector. Note, however, that long-term numerical simulations of the evolution of the elliptic elements of the WIMPs are probably needed to assess the robustness of this prediction, and that for the WIMP spectrum, based on the crude estimate $e \approx 1$. For instance, one expects the actual spectrum $\rho(Q)$ to be a somewhat smoothed version of Figure 2, though the existence of a hump around Q_E should survive.

In view of this uncertainty on the exact spectrum of the WIMP population, we did not compute a precise figure of merit for the indirect neutrino signal from the Earth. Let us only point out the main features of the new signal. First, the capture by the Earth of a slow population $v_X^{\text{new}} \sim v_E$, instead of the standard $v_X^{\text{standard}} \sim v_o$, is more effective. If we take only this effect in account, one would expect a figure of merit of order $(v_o/v_E) \delta_E \sim \rho_1 \sim 1.4 g_{\text{tot}}^{(-10)}$. However, another effect is also quite important. Because of the large ratio $(v_o/v_{\text{escape}}^{\text{Earth}})^2 \sim (220 \text{ kms}^{-1}/11 \text{ kms}^{-1})^2 \sim 400$ the Earth capture probability for incoming standard WIMPs is strongly peaked around the “resonances” $m_X \simeq m_A$ for some element A in the Earth [9]. For the new population $(v_X/v_{\text{escape}}^{\text{Earth}})^2 \sim 9$ is much smaller, and the resonances become much broader. This means in particular that for masses $m_X > m_{56}$ (iron resonance) the neutrino signal will be much amplified, compared to standard expectations. However, the maximum WIMP mass for which capture is important depends very sensitively on the low-velocity cut-off v_c (measured in the Earth frame) of the WIMP population. Indeed, taking into account the fact that the escape velocity from the iron core of the Earth is $v_{\text{esc}}^{\text{Fe}} \sim 15 \text{ kms}^{-1}$, capture is only possible when $\beta_-^{\text{Fe}} \geq (v_c/v_{\text{esc}}^{\text{Fe}})^2$, which defines an upper bound on m_X . For instance, within our present (rough) approximation, $v_c = v_\oplus$ so that only WIMPs with mass $m_X \leq 2.62 m_{\text{Fe}} \simeq 147 \text{ GeV}$ would be captured by the Earth.

VII. ESTIMATES FOR REALISTIC WIMPS

To determine the relevance of the effects discussed here to the ongoing search for halo WIMPs, the actual numerical value of $g_{\text{tot}}^{(-10)}$ for realistic WIMPs is of central importance to consider. To investigate this question we have explored the parameter space of the theoretically best motivated WIMP candidate: the lightest supersymmetric particle (assumed to be a neutralino) of the “Minimal Supersymmetric Standard Model” (MSSM) [5]. Of course this is really not a single model, but a range of models, depending upon the assumptions one makes about such issues as Unification, and also the nature of Supersymmetry breaking. Because of this, detailed specific predictions of remnant neutralino densities, elastic scattering cross sections, etc., are difficult to give with any generality. Indeed, our understanding of SUSY models is still developing, so that predictions of annihilation rates in the early universe, and thus remnant neutralino densities may require alteration [22].

In any case, for the purposes of this investigation it is worth exploring the general order of magnitude of predicted solar capture cross sections, and the resulting solar system density of SUSY WIMPs. To this end, to sample the many SUSY parameters, we have made use of the

specialized code Neutdriver written by Jungman, Kamionkowski and Griest [5]. This allows a calculation, using a specific parameterization of MSSMs, of annihilation rates, remnant neutralino densities, and elastic scattering cross sections on isotopes in the Sun, and in potential terrestrial detectors.

Constraints on the SUSY parameter space are also model dependent, depending on whether one uses various GUT relations for gaugino masses, and also on assumptions about universality of scalar and fermion masses. These constraints are also evolving as new data from LEP, and from such processes as $b \rightarrow s \gamma$ are obtained. At the time the calculations reported here were performed, these constraints led us to sample the SUSY phase space described in Table 1 (conventions are those of Jungman *et al.* [5]).

As implied by the data in Table 1, a total of 9600 different sets of SUSY parameters were initially chosen. Among these some combinations, reported by Neutdriver, were unphysical or phenomenologically unacceptable for a variety of reasons. These were culled, and the remaining allowed configurations were utilized to determine remnant densities and scattering cross sections.

This residual phase space has some characteristics that are important to distinguish here. First, we include neutralino masses as large as 400 GeV. These masses are larger than conventionally displayed in constraints by ongoing direct WIMP detection experiments. However as we are interested here primarily in knowing how broadly relevant our results might be, we wanted to explore as large a region of phase space as possible —independent of model builders’ or experimentalists’ preferences. This factor also played a role in our choice of WIMP cosmic densities to include in this analysis. From the broad phase space that survived the above cuts, we then selected those models that resulted in a remnant density in the range $0.025 < \Omega_X h^2 < 1$. This range again is somewhat broader than is conventionally chosen for Ω . However, given the upper limit $\Omega_{\text{Baryon}} h^2 < .026$ from Big Bang Nucleosynthesis [4] it remains possible that the non-baryonic abundance could be as small as the lower bound quoted above and still at least marginally exceed the baryon density in our own galaxy. This relaxed choice of density restriction, combined with the higher mass range we consider, implies that we allow models with somewhat higher cross sections on terrestrial targets than is usually displayed when SUSY constraint diagrams are displayed. (It is generally true, for example, that those models with the lowest remnant density today have the highest elastic scattering cross sections, for reasons made clear in the introduction to this paper.). In any case, the results quoted here are meant to be indicative of what one might expect for realistic WIMPs, and since SUSY model predictions are themselves evolving, the detailed model results quoted here should be taken as indicative of the general order of magnitude of one’s expectations for SUSY WIMPs. Nevertheless, in order to explore how restricting the remnant neutralino density will affect the range of g ’s expected for SUSY WIMPs, we also considered subset of the parameter space in which $0.1 < \Omega_X h^2 < 1$.

Each neutralino has two possible modes of scattering on targets, in both the Sun and in terrestrial detectors. Because neutralinos are Majorana particles the non-relativistic limit of the scattering cross section generically involves a spin-dependent piece. In addition, exchange of scalar particles can produce a scalar, spin-independent piece. This latter term, if present, generally dominates for large nuclear targets, because in this case the WIMP can scatter coherently off of the entire nucleus with a coupling proportional to the atomic number of the nucleus A . Thus the cross section goes as A^2 . Moreover, the cross section generically

involves as factor the square of the WIMP-nucleus reduced mass, $(m_A m_X / (m_A + m_X))^2$, which, for heavy WIMPs, also increases as the square of the mass of the target nuclei. Since this latter quantity is also proportional to A , this implies that the scattering cross section for heavy nuclei can include a factor proportional to A^4 , which for nuclei as heavy as iron or germanium can be very large indeed.

As a result, one generically finds that scattering cross sections are dominated by the coherent scalar piece in all cases except where this piece is suppressed due to various model-dependent factors. Moreover, with the exception of hydrogen and nitrogen, all other nuclei in the Sun are even-even nuclei, and for these nuclei the spin-dependent amplitude vanishes. In calculating the solar capture rate described in this paper, we included all known elements in the Sun, with abundances given by current solar model calculations. All elemental abundances except for hydrogen and helium are taken from Jungman *et al.* [5] while the former two abundances are taken from Bahcall and Pinsonneault [18]. We display the mass fractions used for the various elements in Table 2.

In addition to calculating the capture factors g_A , we also determined the scattering cross sections on germanium, which is currently the target material of choice in cryogenic detectors. In order to express the results in a more target independent way, however, we adopt a standard presentation of this cross section in terms of the effective WIMP-nucleon cross section. This is obtained by scaling from targets of atomic number A , using the assumption of coherent scattering, and is given by:

$$\sigma_p \equiv \frac{\sigma_A}{A^2} \left(\frac{m_X + m_A}{m_X m_A} \right)^2 \left(\frac{m_X m_p}{m_X + m_p} \right)^2 \simeq \frac{\sigma_A}{A^4} \frac{(m_X + m_A)^2}{(m_X + m_p)^2}. \quad (7.1)$$

We present our results in Tables 3 and 4 and Figures 3-6. In the tables, in addition to the value of $g_{\text{tot}}^{(-10)}$, we also display the value of $g_{\text{H,scalar}}^{(-10)}$, $g_{\text{Fe}}^{(-10)}$, and $g_{\text{O}}^{(-10)}$. In the figures we display WIMP-Nucleon effective cross sections as a function of mass for different models, where models with $\mu > 0$ ($\mu < 0$) are displayed in odd (even) figures. The size of the model point gives the range of the value of $g_{\text{tot}}^{(-10)}$ calculated for this model. The different figures refer to different cutoff values for the WIMP remnant cosmic density. In the figures we also show approximate limits obtained from direct detection experiments on σ_p [23] under two assumed values for the local halo WIMP density ($\rho = 0.3 \text{ GeV cm}^{-3}$ and $\rho = 0.1 \text{ GeV cm}^{-3}$).

Several features should be clear from these results. First, g_{tot} values in excess of unity are clearly possible, implying that realistic WIMPs to which the next generation of direct detectors will be sensitive should be expected to have a solar-system density in the region of the Earth that is significant. Second, we note that there is in general a monotonic relation between σ_p and g_{tot} , with however, wide dispersion. Approximately one has

$$g_{\text{tot}}^{(-10)} \sim \sigma_p / (6 \times 10^{-41} \text{ cm}^2). \quad (7.2)$$

Also note that in this case, the dominant single contribution to g_{tot} comes from scattering on iron in the Sun, although the net contribution to g_{tot} from the combination of lighter elements is of the order of 40% of the total. For $\mu < 0$, an additional possibility arises, at least for the lowest values of $\Omega_X h^2$ and for low mass WIMPs. In this case, solar capture can be dominated by spin-dependent scattering off hydrogen so that the germanium cross

section, and hence the effective σ_p can be several orders of magnitude smaller than in the case of WIMPs for which the dominant scattering on heavy nuclei is coherent.

As one increases the lower limit on the remnant WIMP cosmic density today, several effects ensue. First, as expected, increasing this lower cutoff tends to decrease the mean value of g_{tot} . Also, for $\mu < 0$ the low mass low σ_p branch of WIMP phase space rapidly decreases in size, disappearing completely by the time the cutoff on Ωh^2 exceeds 0.1. Thus, if the cosmic density exceeds this value, then a large solar system population is in one to one correspondence with WIMPs that should be directly detectable in the next generation of detectors.

Finally, we have examined what would be the effect of changing the average velocity dispersion of halo WIMPs. We considered a range $180 < v_o < 270$, which encompasses most estimates for this quantity for our galactic halo, and found that the results in all cases changed by less than 10% compared to those quoted above. It is interesting that while the change was too slight to be significant, the direction of the change was not monotonic, but depended upon the mass of the WIMP and the dominant target atom in the Sun. For heavy WIMPs whose dominant scattering was on heavy elements, increasing v_o increased the capture factor g_{tot} .

VIII. CONCLUSIONS

The results presented here are quite encouraging, and motivate a consideration of detection schemes that might probe down to keV energy deposits by WIMP scattering. If this is possible, the observation of a rise in the differential event rate for low energy events, of the form we describe here, could provide a very useful discriminant that could demonstrate that any claimed WIMP signal at higher energy is, in fact, due to halo WIMPs. While it is challenging to consider obtaining sensitivity to such low energy events (and more importantly reducing the background of noise for such events), this may be less daunting than attempting to achieve directional sensitivity, which is the alternative discriminant that has been discussed [24,25]. Of course, if one had directional sensitivity, the signal we discuss here should be even easier to disentangle from backgrounds, as we expect it should be extremely anisotropic, as described earlier.

Nevertheless, the analytical results presented here are in some sense still preliminary. While we expect the general quantitative features of this new WIMP population will be well approximated by the results presented here, full scale numerical simulations of the WIMP orbits under consideration will be necessary to confirm the details of our results. In particular, knowledge of the anisotropy of the distribution, as well as its energy spectrum will require such simulations, and the results presented here should be considered qualitative in these regards. In addition, such simulations, which incorporate the presence of the planets and allow close encounters, will be necessary to confirm that the WIMP population we focus on here is indeed long-lived in the solar system, and that its spatial distribution is not critically different from the simple spherically symmetric, high-eccentricity one we have assumed.

One area that has not been investigated in detail here, and which certainly warrants further investigation, is the implications of this new distribution for indirect WIMP detection

via annihilations in the Earth. As we described in the text, it is quite likely that this signal could be significantly enhanced, especially for heavy WIMPs, compared to that which is calculated for halo WIMP capture by the Earth. We expect, in fact, that new bounds on SUSY phase space may be possible on the basis of such considerations, compared to existing limits from underground neutrino detectors. Such an investigation is currently underway.

ACKNOWLEDGMENTS

We thank G. Jungman for kindly providing us with a copy of the code Neutdriver. The hospitality of CERN, where this work was initiated, is gratefully acknowledged. LMK thanks the colleagues at CERN for discussion on SUSY limits from LEP. In addition, he thanks the IHES for hospitality during the completion of this project. We thank Andrew Gould for suggesting a simplified derivation of Eq. (2.22). We also wish to thank D. Devaty and P. Kernan for significant programming support and for discussions, and the anonymous referee for constructive and insightful comments. LMK's research is supported in part by the DOE.

REFERENCES

- [1] V. Trimble, *Annu. Rev. Astron. Astrophys.* **25**, 425 (1989);
K.M. Ashman, *Proc. Astron. Soc. Pac.* **104**, 1109 (1992).
- [2] D. Tytler, X. M. Fan, and S. Burles, *Nature*, **381**, 207 (1996)
- [3] C. Copi, D.N. Schramm, and M.S. Turner, *Science*, **267**, 192 (1995)
- [4] L. M. Krauss and P. J. Kernan, *Phys. Lett.* **B347**, 347 (1995)
- [5] G. Jungman, M. Kamionkowski and K. Griest, *Phys. Rep.* **267**, 195 (1996)
- [6] E.W. Kolb and M.S. Turner, *The early universe* (Addison-Wesley, Redwood City, 1990).
- [7] T. Damour and L.M. Krauss, astro-ph/9806165 (1998)
- [8] L. M. Krauss *et al*, *Ap. J.* **299**, 1001 (1985)
- [9] A. Gould, *Astrophys. J.* **321**, 571 (1987).
- [10] A. Gould, *Astrophys. J.* **388**, 338 (1992).
- [11] L. Landau and E. Lifshitz, *Mechanics* (Pergamon Press, Oxford, 1982).
- [12] D.N. Spergel and W.H. Press, *Astrophys. J.* **294**, 663 (1985).
- [13] D. Brouwer and G.M. Clemence, *Methods of Celestial Mechanics* (Academic Press, Orlando, 1961).
- [14] Y. Kozai, *The Astronomical Journal* **67**, 591 (1962)
- [15] V. Béletsky , *Essais sur le mouvement des corps cosmiques*, Editions Mir, Moscow (1986).
- [16] F. Thomas and A. Morbidelli, *Celestial Mechanics and Dynamical Astronomy* **64**, 209 (1996)
- [17] M. Holman, J. Touma, and S. Tremaine, *Nature* **386**, 254 (1997)
- [18] J.N. Bahcall and M.H. Pinsonneault, *Rev. Mod. Phys.* **64**, 885 (1992).
- [19] B.J. Gladman *et al*, *Science* **277**, 197 (1997)
- [20] A. Morbidelli and C. Froeschlé, in *Impacts in the Solar System*, D. Benest and C. Froeschlé, eds., (Proceedings of the Goutelas School, 1994), pp. 1-25.
- [21] R. Greenberg and M. Nolan, in *Resources of Near-Earth Space*, J. Lewis, M.S. Matthews and M.L. Guerrieri, eds. (Univ. Arizona Press, Tucson, 1993), pp. 473-492.
- [22] G. Kane, to appear in *Phys. Rep.*, Proceedings of UCLA Workshop on Sources and Detection of Dark Matter, D. Cline, ed., in press (1998)
- [23] see, for example M. Beck *et al*, *Phys. Lett. B* **336**, 141 (1994); D. S. Akerib *et al.*, astro-ph/9712343; L. Bergé *et al.*, astro-ph/9801199; A. Bottino *et al*, *Phys. Lett. B* **402**, 113 (1997). See also R. Bernabei *et al*, *Phys. Lett. B* **389**, 757 (1996) (note that we do not utilize the most recent quoted limit of this group as this limit is still somewhat controversial).
- [24] D. N. Spergel, *Phys. Rev. D* **37** 3495 (1988)
- [25] see L.M. Krauss, to appear in *Phys. Rep.*, Proceedings of UCLA Workshop on Sources and Detection of Dark Matter, D. Cline, ed., in press (1998), and refs therein.

TABLES

$\mu < 0$	M_2 : 80-800 GeV	(10 steps)
	M_1, M_3 determined by GUT relations	
	μ : -800 - -60 GeV	(10 steps)
	$\tan\beta$: 2 -40	(4 steps)
	m_A : 70 -500 GeV	(3 steps)
	m_{squark}^2 : $4 - 64 \times 10^4 \text{ GeV}^2$	(4 steps)
$\mu > 0$	M_2 : 80-800 GeV	(10 steps)
	M_1, M_3 determined by GUT relations	
	μ : 150 - 800 GeV	(10 steps)
	$\tan\beta$: 2 -40	(4 steps)
	m_A : 70 -500 GeV	(3 steps)
	m_{squark}^2 : $4 - 64 \times 10^4 \text{ GeV}^2$	(4 steps)

TABLE I. SUSY Parameter Space Sampled in Estimates

Element	Atomic Mass Number	Mass Fraction
H	1	0.7095
He	4	0.2715
C	12	3.87×10^{-3}
N	14	9.40×10^{-4}
O	16	8.55×10^{-3}
Ne	20	1.51×10^{-3}
Mg	24	7.39×10^{-4}
Si	28	8.13×10^{-4}
S	32	4.65×10^{-4}
Fe	56	1.46×10^{-3}

TABLE II. Elemental Mass Fractions Used in Solar Capture Estimates

	Ωh^2	$m_X(\text{GeV})$	g_{tot}	g_H	g_O	g_{Fe}	σ_p
$\mu > 0$							
	0.037	384	2.480	0.008	.410	1.532	1.38E-40
	0.038	384	2.239	0.007	.370	1.381	1.25E-40
	0.036	384	2.219	0.007	.367	1.370	1.24E-40
	0.032	306	1.943	0.008	.354	1.136	1.27E-40
	0.029	306	1.886	0.007	.342	1.103	1.24E-40
	0.027	306	1.871	0.007	.340	1.094	1.22E-40
	0.076	353	1.230	0.004	.210	.746	7.28E-41
	0.074	353	1.173	0.004	.201	.710	6.94E-41
$\mu < 0$							
	0.039	357	0.63	0.002	0.11	0.38	3.70E-41
	0.039	357	0.61	0.002	0.10	0.37	3.55E-41
	0.038	357	0.60	0.002	0.10	0.37	3.53E-41
	0.025	32	0.59	0.000	0.00	0.00	8.17E-44
	0.037	276	0.59	0.002	0.11	0.34	4.16E-41
	0.035	276	0.58	0.002	0.11	0.33	4.08E-41
	0.034	276	0.58	0.002	0.11	0.33	4.08E-41
	0.029	196	0.55	0.003	0.12	0.29	5.12E-41

TABLE III. Largest $g_{\text{tot}}^{(-10)}$ values for $0.1 > \Omega_X h^2 > 0.025$

	Ωh^2	$m_X(\text{GeV})$	g_{tot}	g_H	g_O	g_{Fe}	σ_p
$\mu > 0$							
	0.135	397	1.11	0.003	0.18	0.69	6.06E-41
	0.150	80	0.97	0.013	0.23	0.47	2.07E-40
	0.126	80	0.96	0.013	0.23	0.47	2.06E-40
	0.211	80	0.86	0.012	0.20	0.42	1.84E-40
	0.143	397	0.74	0.002	0.12	0.46	4.07E-41
	0.136	397	0.74	0.002	0.12	0.46	4.04E-41
	0.110	316	0.64	0.002	0.12	0.38	4.10E-41
	0.103	316	0.62	0.002	0.11	0.37	3.97E-41
	0.165	359	0.46	0.002	0.08	0.28	2.69E-41
	0.170	359	0.43	0.001	0.07	0.26	2.54E-41
	0.164	359	0.43	0.001	0.07	0.26	2.50E-41
	0.123	396	0.39	0.001	0.06	0.24	2.14E-41
	0.124	278	0.37	0.002	0.07	0.21	2.63E-41
$\mu < 0$							
	0.101	361	0.26	0.001	0.04	0.16	1.49E-41
	0.104	361	0.24	0.001	0.04	0.15	1.40E-41
	0.107	199	0.21	0.001	0.04	0.11	1.92E-41
	0.148	402	0.18	0.001	0.03	0.11	9.61E-42
	0.149	402	0.18	0.001	0.03	0.11	9.53E-42
	0.130	321	0.18	0.001	0.03	0.10	1.10E-41
	0.135	321	0.17	0.001	0.03	0.10	1.06E-41
	0.134	321	0.17	0.001	0.03	0.10	1.06E-41
	0.168	362	0.16	0.001	0.03	0.10	9.17E-42
	0.169	240	0.16	0.001	0.03	0.09	1.24E-41

TABLE IV. Largest $g_{\text{tot}}^{(-10)}$ values for $1.0 > \Omega_X h^2 > 0.1$

FIGURES

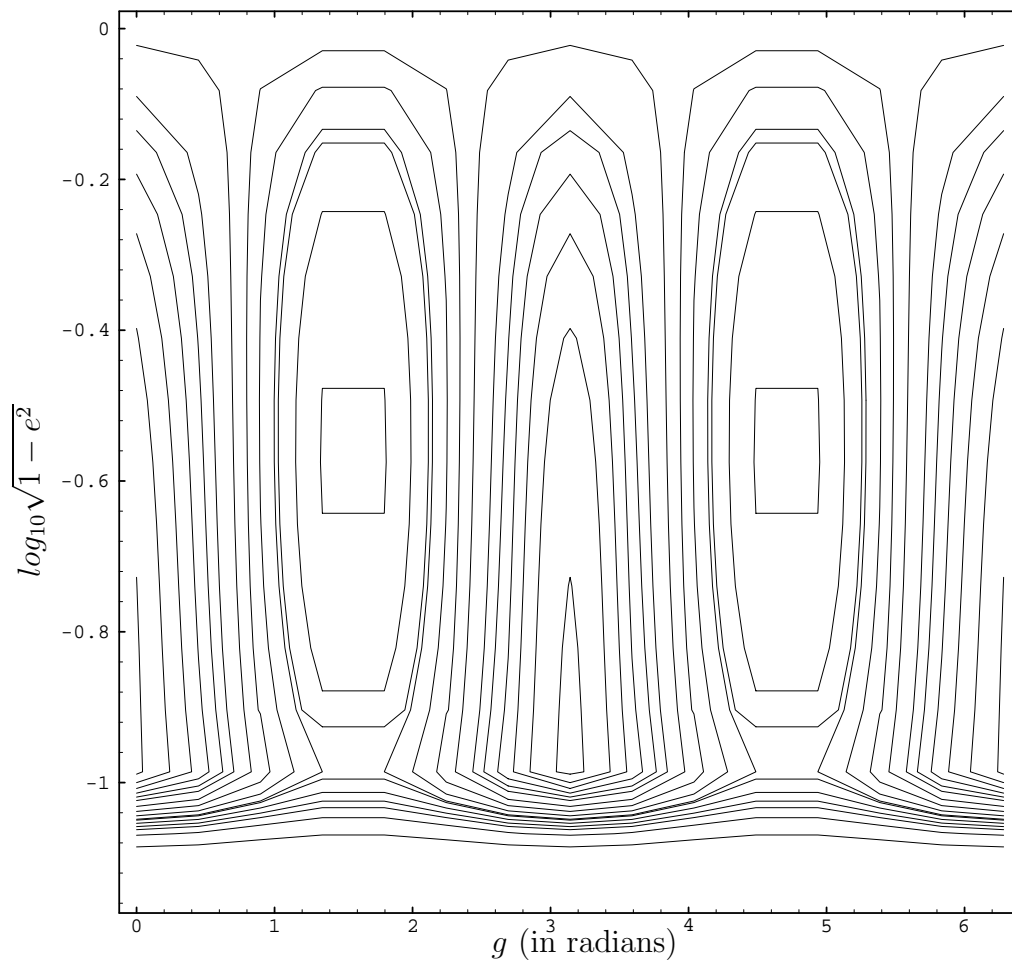


FIG. 1. Level curves of the perturbation Hamiltonian describing the secular evolution of the canonical pair (G, g) . Note the divide between trajectories that always stay within the Sun and those that get out.

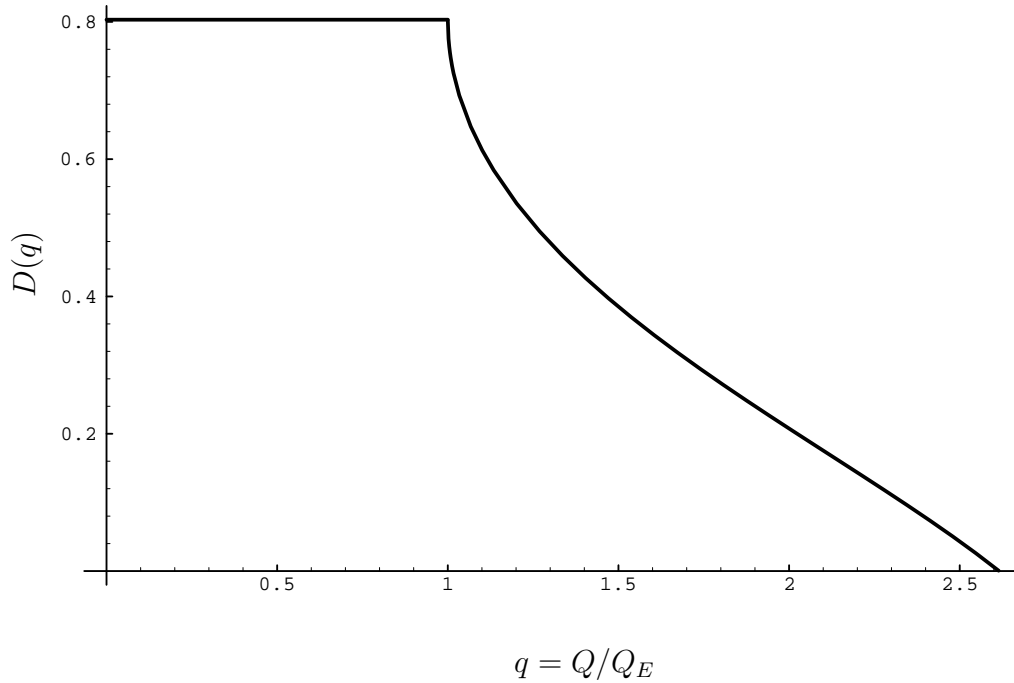


FIG. 2. Shape of the differential rate (per keV) of the additional scattering events caused by the WIMP population considered here. This figure represents the function $D(q)$, where $q = Q/Q_E$ is the energy transfer in units of the characteristic energy scale Q_E (in the keV range).

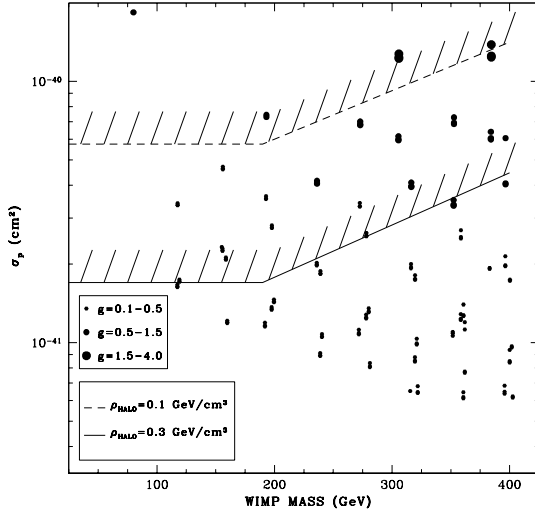


FIG. 3. g_{tot} as a function of the effective WIMP nucleon cross section, σ_p , and WIMP Mass, for $\mu > 0$, and assuming $\Omega_X h^2 > 0.025$. Hatched curves represent experimental upper limits assuming $\rho = 0.3 \text{ GeV cm}^{-3}$ (lower) and $\rho = 0.1 \text{ GeV cm}^{-3}$ (upper).

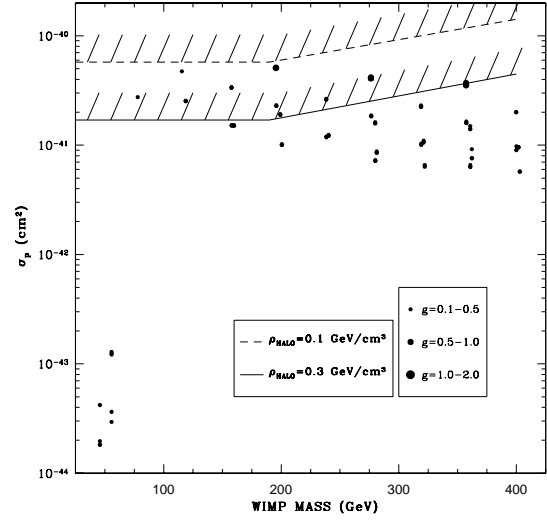


FIG. 4. Same as Figure 3 but with $\mu < 0$

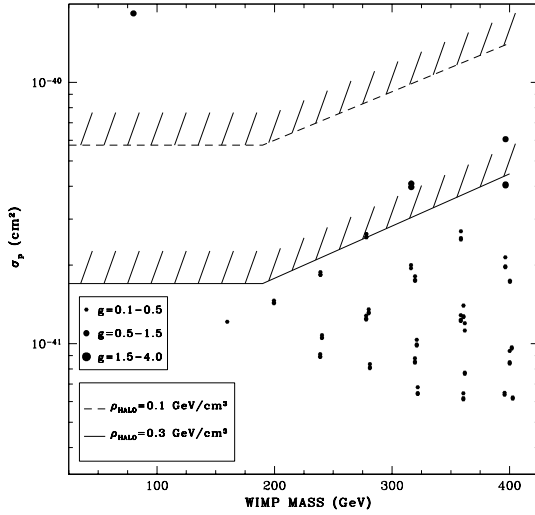


FIG. 5. Same as Figure 3, but assuming $\Omega_X h^2 > 0.1$

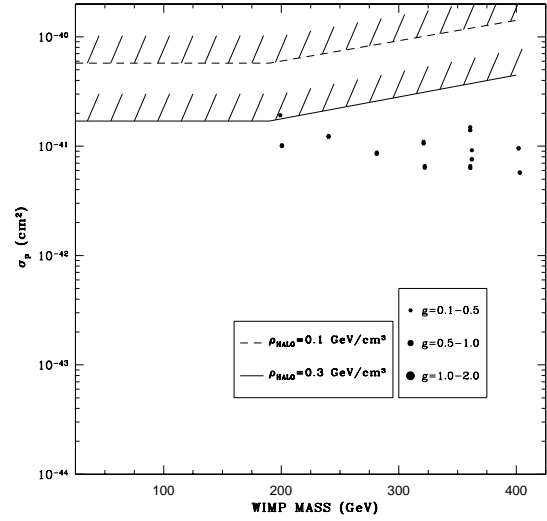


FIG. 6. Same as Figure 5, but with $\mu < 0$